

**USEE 2001: Utility Software for Earthquake Engineering
Report and User's Manual**

Mid America Earthquake Center

Mehmet Inel, Erich M. Bretz, Edgar F. Black,
Mark A. Aschheim, and Daniel P. Abrams

Civil and Environmental Engineering
University of Illinois at Urbana-Champaign
Urbana, Illinois

October 2001

ACKNOWLEDGMENTS

The Mid-America Earthquake Center is a National Science Foundation Center for Earthquake Engineering. Synthetic ground motions distributed with USEE were developed by Y. K. Wen and Chiun-Lin Wu as part of project RR-1 of the Mid-America Earthquake Center (1999). Previous work by Mahin and Lin (1983), which included a variable time step algorithm developed by Professor R. Klingner of the University of Texas at Austin, Abrams (1985), and Boroschek and Mahin (1991), was used in the development of this software.

This work was supported primarily by the Mid America Earthquake Center under the Earthquake Engineering Research Centers Program of the National Science Foundation under Award Number EEC-9701785.

Windows 95, Windows 98, Windows 2000, Windows NT 4.0, and Microsoft Word are registered trademarks of the Microsoft Corporation.

TERMS AND DISCLAIMER

Considerable time, effort, and expense have gone into the development and documentation of Utility Software for Earthquake Engineering (USEE). The program has been thoroughly tested and used. However, no warranty of any kind, express or implied, is made with respect to the USEE software product, and specifically, no warranty is made that USEE is merchantable or fit for any particular purpose. Any description of USEE shall not be deemed to create an express warranty that USEE conforms to this description.

Receiver assumes all risk and liability for loss, damage, claims, or expense resulting from use, possession, or distribution of any software products furnished by the developer. Receiver agrees to indemnify, defend, and hold harmless the developer, its officers, agents, and employees from and against any and all claims, liability, loss, damage, or expense, including reasonable attorney's fees, arising from or by reason of receivers' use, possession, or distribution with respect to any of the software products furnished by the developer and such obligation shall survive acceptance of said products therefore by receiver. Receiver agrees that it will not resell the software products furnished hereunder, although free distribution to others is permitted.

CONTENTS

1	Introduction	1
1.1	Program Description	1
1.2	Document Overview	2
1.3	Typographical Conventions	2
2	Theoretical Basis	4
2.1	Response of SDOF Systems.....	4
2.1.1	Theoretical Formulation.....	4
2.1.2	Energy Terms	4
2.1.3	Computational Aspects	6
2.2	Single-Degree-of-Freedom Analogies of Multistory Buildings.....	11
2.2.1	The “Equivalent” Single-Degree-of-Freedom System	11
2.2.2	Implementation of the SDOF Analogue in USEE.....	16
2.3	Computation of Response Spectra Using USEE.....	17
2.3.1	Specification of Periods	18
2.3.2	Computation of Elastic Response Spectra	18
2.3.3	Computation of Inelastic Response Spectra.....	19
3	User’s Manual	23
3.1	Installing and Maintaining the Program	23
3.1.1	USEE Distribution	23
3.1.2	Hardware Recommendations	23
3.1.3	Un-installation Guide.....	23
3.1.4	Maintenance and Support.....	23
3.2	Program Design	24
3.2.1	Module Operation	24
3.2.2	Directory Structure	24
3.3	Using the Program.....	25
3.3.1	Description of Commands.....	25
3.3.2	User Preferences	27
3.3.3	SDOF Analysis Steps.....	28
3.3.4	Multistory Building Approximation Analysis Steps	29
3.3.5	Response Spectra Analysis Steps	29
3.3.6	Windows Copy & Paste	30
3.3.7	Input and Output Data Files	30
3.3.8	Summary Data Files.....	31
3.4	Modeling and Response Computation.....	31
3.4.1	Load-Deformation Models.....	31
3.4.2	Load-Deformation Curve Properties	34
3.4.3	Response Spectra Parameters	37
3.5	Base Motion Input	37
3.5.1	Recorded Ground Motions	37
3.5.2	Synthetic Motions	39
3.5.3	Pulses	41
3.5.4	Scale Factors.....	43
3.6	Tutorial.....	43
3.6.1	SDOF Analysis Example	43

3.6.2	Multistory Building Approximation Analysis Example	46
3.6.3	Response Spectra Examples	47
4	Program Verification	52
4.1	Accuracy of Computational Engine.....	52
4.2	Accuracy of Multistory Building Approximation Analysis: Example	54
	APPENDIX A: Software Development Tools	60
	APPENDIX B: Algorithm for Computing Isoductile Response Spectra.....	61
B.1	Introduction	61
B.2	Properties of the Strength-Ductility Relationship	61
B.3	Description of the Algorithm	65
B.3.1	Initial Bounding of Solution.....	66
B.3.2	Fast Search Bisection.....	71
B.4	Comparison of Results with Other Programs.....	73
B.4.1	Accuracy of Constant Ductility Response Spectra.....	74
B.4.2	Computational Efficiency	75
B.5	Conclusion.....	77
B.6	Glossary/Definitions	77
	APPENDIX C: Notation	78
	APPENDIX D: USEE Organization.....	81
	APPENDIX E: References	83

TABLES

Table 1.	Constant ductility algorithm parameters	22
Table 2.	Response quantities available for export	31
Table 3.	Validation of SDOF code	52
Table 4.	First elastic mode shape of the 12-story building frame	57
Table B1.	Ground motions used in the computations	74
Table B2.	Clock time required to compute response spectra for different ductilities using different software programs	76

FIGURES

Figure 1.	SDOF system subjected to ground acceleration	4
Figure 2	Schematic illustration of absorbed energy for an oscillator with a bilinear load-deformation relationship.	6
Figure 3.	Effect of convergence tolerance on (a) overshoot during loading and (b) hysteretic response on unloading	10
Figure 4.	Establishing the properties of an “equivalent” SDOF system: (a) capacity curve determined from the nonlinear static (pushover) analysis of the building, (b) load-deformation curve of the SDOF analogue, derived from the capacity curve	16
Figure 5.	Default mode shapes available in USEE	17
Figure 6.	Linear elastic model	32
Figure 7.	Bilinear model.....	33
Figure 8.	Stiffness-degrading model.....	34
Figure 9.	Load-deformation response of a bilinear oscillator with (a) positive post-yield stiffness, (b) negative post-yield stiffness.....	37
Figure 10	Pulse types	42
Figure 11.	SDOF example: Base Shear / Weight vs. Displacement (cm).....	45
Figure 12.	SDOF example: Displacement (cm) vs. Time (sec).....	45
Figure 13.	Multistory building approximation example: Base Shear / Weight vs. Roof Displacement (cm)	47
Figure 14.	Multistory building approximation example: Roof Displacement (cm) vs. Time (sec)	48
Figure 15.	Response spectra example: Spectral Acceleration (g) vs. Period (sec).....	49
Figure 16.	Response spectra example: Ductility vs. Period (sec).....	50
Figure 17.	Yield Point Spectra: Base Shear / Weight vs. Period (sec)	51
Figure 18.	Yield Point Spectra: Base Shear / Weight vs. Yield Displacement (cm)	51
Figure 19.	Comparison of USEE to NONLIN and NONSPEC: Displacement (cm) vs. Time (sec)	53
Figure 20.	Comparison of USEE to NONLIN and NONSPEC: Force vs. Displacement (cm)	54
Figure 21.	Multistory building approximation analysis example.....	55
Figure 22.	First elastic mode shape of the 12-story building frame	58
Figure 23.	Capacity curve obtained by applying forces proportional to the product of the elastic modal amplitude and mass at each floor in a nonlinear static (pushover) analysis.....	58
Figure 24.	Displacement history of a 12-story building frame subjected to 1940 El Centro record (amplitude scaled by factor of 2)	59
Figure 25.	Base shear vs. roof displacement response of the 12-story building frame subjected to 1940 El Centro record (amplitude scaled by factor of 2).....	59
Figure B1.	(a) Schematic load-deformation response, and (b) normalized load-deformation response	62
Figure B2.	Computed load-deformation response to 1992 Landers earthquake at Joshua Tree Fire Station (NS), for a 1-second period oscillator	63
Figure B3.	The strength-ductility relationship for a bilinear oscillator having a period of $T= 0.15$ sec responding to the 1987 Whittier Narrows record.....	63

Figure B4.	The strength-ductility relationship for a bilinear oscillator responding to the 1987 Whittier Narrows record for an oscillator period of: (a) 0.20 sec, and (b) 0.15 sec.....	65
Figure B5.	Linear interpolation between $C_{y,u}$ and $C_{y,l}$	66
Figure B6.	The first phase of the algorithm, for determining the initial bounds on the solution	67
Figure B7.	The case where $\mu(C_{y,e}) > \mu_t$	68
Figure B8.	The case where $\mu(C_{y,e}) < \mu_t$	69
Figure B9.	Definition of smoothness ratio (e/a), in the context of checking an interval for rejection.....	70
Figure B10.	Checking for a possible solution in the check-reject region.....	71
Figure B11.	Bisection with the “fast search” algorithm	72
Figure B12.	Constant ductility response spectrum for $\mu= 2$ for the El Centro record	75
Figure B13.	Constant ductility response spectrum for $\mu= 2$ for the Llole record	75

1 Introduction

Utility Software for Earthquake Engineering (USEE) provides a Windows-based user-friendly graphic interface for performing simple computer simulations of the response of structures subjected to earthquake ground shaking and for accessing data and products of the Mid-America Earthquake Center. The visual interface allows students, practicing engineers, and researchers to quickly simulate nonlinear dynamic response and to understand the influence of parameter variations on response characteristics. Because the results are easily obtained using a “point and click” interface, USEE makes it possible to easily master the richness and variety of response that may be developed as parameters are varied. This understanding is increasingly important as greater attention is given to the seismic performance of new and existing structures in education, research, and practice.

1.1 Program Description

The USEE interface makes nonlinear analysis nearly effortless. The user is guided through several data input screens. A point-and-click interface allows the user to navigate through the menus and to select analysis options. Simulated response is displayed using versatile plots that allow the user to select among a variety of response parameters to be plotted. Response data is summarized on screen and may be saved as ASCII text files for subsequent processing. Response plots may be copied to the Windows clipboard and then pasted into Windows applications (e.g. Microsoft Word) using the **Copy** and **Paste** functions, accessed via a right mouse click. An icon on-screen directs the user’s web browser to load the Mid-America Earthquake Center home page, where current USEE release information as well as research results and other products of the Mid-America Earthquake Center may be obtained, in addition to information about the Mid-America Earthquake Center.

The program includes modules that provide for several kinds of analyses:

- The *Single-Degree-Of-Freedom* (SDOF) analysis module determines the detailed response history of nonlinear single-degree-of-freedom structures.
- The *Multistory Building Approximation* analysis module uses an “equivalent” SDOF representation of the building to estimate the displacement response history of multistory buildings.

- The *Response Spectra* module computes linear and nonlinear response spectra for a range of parameter values.

These capabilities are described further in Section 3.3.

The analyses may be conducted with any of the following load-deformations models:

- linear
- bilinear
- stiffness-degrading

Properties of the oscillator such as period of vibration, viscous damping, yield strength, and post-yield stiffness may be specified by the user. Further details are provided in Section 3.4.

The analyses may be done using base input accelerations selected from the following categories:

- recorded ground motions
- synthetic motions
- pulse waveforms

The program is distributed with a basic complement of motions in these categories, as described in Section 3.5. Users may add additional accelerograms of their choosing to the recorded ground motions category. Accelerogram formatting requirements are described in Section 3.5.

1.2 Document Overview

This report describes:

- capabilities of the USEE program (Chapter 1)
- the theoretical basis of the program (Chapter 2)
- use of the program, its organization, and base motion file formats (Chapter 3)
- validation of the accuracy of the USEE program using several test cases (Chapter 4)

It is recommended that the reader install the USEE software and use it in conjunction with the reading of this report.

1.3 Typographical Conventions

Throughout this manual the following typographical conventions are used. Roman type is used throughout this report unless otherwise noted. Commands and command

buttons are in bold type (e.g., **Export Output**). References to USEE modules and features are in italic type (e.g., *Approximate Multistory Building*). Computer directory names are in bold type (e.g., **USEE\Waveforms\Recorded**). Individual file names (such as ground motion records) are in capital letters (e.g., C02_01S.MAE). Arial type is used for ground motion file header data. Variables in equations are in italics (e.g., S_a), matrices and vectors are in bold type (e.g., **Q**), and variables that are represented using Greek symbols are shown in regular text (e.g., Γ).

2 Theoretical Basis

2.1 Response of SDOF Systems

2.1.1 Theoretical Formulation

The equation of motion for a viscously-damped single-degree-of-freedom system subjected to ground acceleration $\ddot{u}_g(t)$ (see Figure 1) is given as a function of time, t , by:

$$M\ddot{u}(t) + C\dot{u}(t) + R(t) = -M\ddot{u}_g(t) \quad (1)$$

where M = mass of the system, C = viscous damping coefficient, $R(t)$ = restoring force, and $\ddot{u}_g(t)$ = ground acceleration. The term $u(t)$ is the displacement of the system relative to the ground and represents the deformation of the structure, while $u_g(t)$ is the displacement of the ground relative to a fixed datum. The total displacement of the system is given as $u^i(t) = u(t) + u_g(t)$. By taking derivatives with respect to time, the absolute acceleration $\ddot{u}^i(t)$ is $\ddot{u}^i(t) = \ddot{u}(t) + \ddot{u}_g(t)$. The restoring force for a linear elastic system is given as $R(t) = Ku(t)$ where K is the stiffness. For a nonlinear system, $R(t)$ is determined as a function of the current deformation, $u(t)$, as represented by the load-deformation relationship.

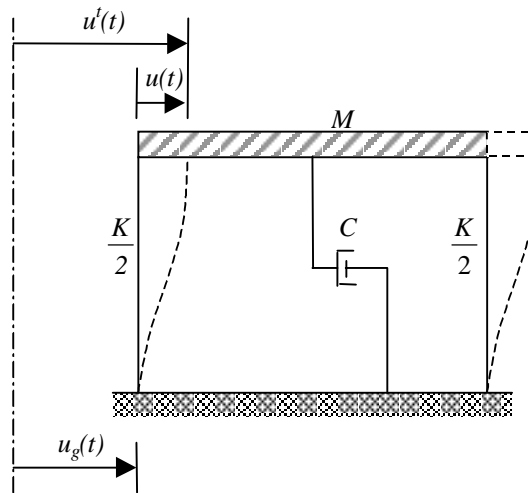


Figure 1. SDOF system subjected to ground acceleration

2.1.2 Energy Terms

Input energy may be computed by integrating the force terms of the equation of motion with respect to the relative displacement of the oscillator. Two equivalent forms of the equation of motion exist:

$$m\ddot{u}'(t) + c\dot{u}(t) + R(t) = 0 \quad (2)$$

$$m\ddot{u}(t) + c\dot{u}(t) + R(t) = -m\ddot{u}_g(t) \quad (3)$$

Integration of the terms of these equations with respect to the relative displacement of the oscillator leads to two different energy relationships (Uang and Bertero, 1988). The integration of Eq. 2 leads to the so-called “absolute” energy equation, while integration of Eq. 3 leads to the so-called “relative” energy equation. USEE computes relative energy quantities.

The energy imparted to the SDOF oscillator, known as the “relative input energy,” is given by integration of the right-hand term of Eq. 3:

$$E_i = -\int_0^u m\ddot{u}_g(t) du \quad (4)$$

The relative input energy, E_i , represents that work done by the equivalent lateral force ($-m\ddot{u}_g$) moving through the relative displacements of the oscillator. The relative input energy is ultimately dissipated through damping and hysteretic losses. The dynamic portion of the response also contains kinetic energy associated with the relative velocity of the mass and potential energy associated with the elastic strain energy.

The “relative” kinetic energy, E_k , of the mass, obtained by integrating the first term of Eq. 3 (Uang and Bertero, 1988) is

$$E_k = \int_0^u m\ddot{u}(t) du = \frac{m\dot{u}^2}{2} \quad (5)$$

The energy dissipated by viscous damping, E_ξ , given by integration of the second term of Eq. 3, is

$$E_\xi = \int_0^u c\dot{u}(t) du = \int_0^t c[\dot{u}(t)]^2 dt \quad (6)$$

The energy absorbed by the oscillator is composed of recoverable elastic strain energy, E_s , and irrecoverable hysteretic energy, E_h . These are obtained by integrating the third term of Eq. 3:

$$E_a = \int_0^u R(u) du = E_s + E_h \quad (7)$$

where

$$E_s = \frac{[f_s(t)]^2}{2K} \quad (8)$$

where K = the initial elastic stiffness of the oscillator. The recoverable strain energy,

E_s , and the dissipated hysteretic energy, E_h , are shown schematically in Figure 2 for a bilinear oscillator.

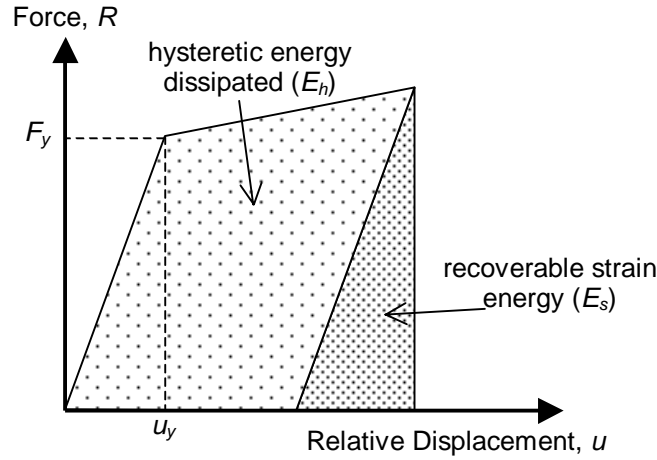


Figure 2. Schematic illustration of absorbed energy for an oscillator with a bilinear load-deformation relationship.

Thus,

$$E_i = E_k + E_\zeta + E_a = E_k + E_\zeta + E_s + E_h \quad (9)$$

USEE allows each of these quantities to be exported. In the *View Results* step of the *Single-Degree-of-Freedom* analysis and *Multistory Building Approximation* module, the quantities are plotted with kinetic and strain energy combined.

2.1.3 Computational Aspects

Closed-form solutions of the equation of motion of a single-degree-of-freedom oscillator are not available for a general nonlinear system and for excitations that vary arbitrarily with time. Solutions may be obtained by numerical integration of the equation of motion in a sequence of step-by-step analyses. Each successive analysis is done over a small time interval for initial conditions determined at the conclusion of the previous time step. The computation for each time interval (Δt) is based on an assumption of the structural characteristics that prevail during the entire time step.

Response during each time interval is computed using the linear acceleration method. The linear acceleration method is a special case of the Newmark Beta Method, with $\alpha = 1/2$ and $\beta = 1/6$. In this method, the response acceleration is assumed to vary linearly during the time step, and the properties of the system are assumed to be invariant during the time step.

For nonlinear systems, a displacement increment near a change in stiffness of the system may result in an imbalance between the dynamic equilibrium determined using the actual properties and the properties assumed during the time step. The equilibrium unbalance is evaluated, and if it is significant, the result for that time step is discarded and a smaller time step is selected. This procedure is applied recursively until the desired level of convergence is achieved. Any remaining unbalance is added to the response acceleration at the end of this time step to enforce dynamic equilibrium. If a reduced time step is used, then after a successful solution is obtained, larger time steps are attempted in subsequent time steps, and the larger time steps are retained if the desired level of convergence is achieved.

2.1.3.1 Incremental Equation of Motion

The equation of motion is presented in terms of time, t , in Eq. 1. In this section, the incremental equation of motion is developed. First, the equation of motion at time $t+\Delta t$ is

$$M\ddot{u}(t+\Delta t)+C\dot{u}(t+\Delta t)+R(t+\Delta t)=P(t+\Delta t) \quad (10)$$

This assumes that the time step (Δt) is small enough such that the system properties remain constant during the time step.

Subtracting Eq.1 from Eq. 10 yields

$$M[\ddot{u}(t+\Delta t)-\ddot{u}(t)]+C[\dot{u}(t+\Delta t)-\dot{u}(t)]+[R(t+\Delta t)-R(t)]=[P(t+\Delta t)-P(t)] \quad (11)$$

Denoting

$$\Delta\ddot{u}(t)=\ddot{u}(t+\Delta t)-\ddot{u}(t) \quad (12a)$$

$$\Delta\dot{u}(t)=\dot{u}(t+\Delta t)-\dot{u}(t) \quad (12b)$$

$$\Delta u(t)=u(t+\Delta t)-u(t) \quad (12c)$$

$$\Delta R(t)=R(t+\Delta t)-R(t) \quad (12d)$$

$$\Delta P(t)=P(t+\Delta t)-P(t) \quad (12e)$$

allows Eq. 11 to be restated as

$$M\Delta\ddot{u}(t)+C\Delta\dot{u}(t)+\Delta R(t)=\Delta P(t) \quad (13)$$

By denoting $\Delta R(t)$ as $K\Delta u(t)$, Eq. 13 may be restated as

$$M\Delta\ddot{u}(t)+C\Delta\dot{u}(t)+K\Delta u(t)=\Delta P(t) \quad (14)$$

where K = tangent stiffness of the structure at time t .

Eq. 14 is the incremental equation of motion, representing conditions required to

maintain dynamic equilibrium during a time step Δt . The linear acceleration method is used to obtain a solution to Eq. 14 over successive time steps Δt . Given the structural properties and motion at time t and the acceleration applied at the base of structure during the time increment Δt , the incremental acceleration $\Delta\ddot{u}(t)$, the incremental velocity $\Delta\dot{u}(t)$, and the incremental displacement $\Delta u(t)$ are computed. The displacement and velocity values at time $t + \Delta t$ are

$$u(t + \Delta t) = u(t) + \Delta u(t) \quad (15a)$$

$$\dot{u}(t + \Delta t) = \dot{u}(t) + \Delta\dot{u}(t) \quad (15b)$$

The acceleration at $t + \Delta t$ is calculated, with a correction for any unbalance in equilibrium,

$$\ddot{u}(t + \Delta t) = \frac{P(t + \Delta t) - C\dot{u}(t + \Delta t) - R(t + \Delta t)}{M} \quad (16)$$

The accuracy and stability of the integration method are important considerations. The linear acceleration method is known to be stable for linear elastic systems only if the time step is less than the period of the system multiplied by 0.551 (e.g. Chopra, 1995). This is described as “conditionally stable” in the literature, because the stability of the solution is assumed only under the condition that a small enough time step is used. However, the stability limit is not restrictive in practice because the time step must be considerably smaller than this limit to ensure adequate accuracy in the numerical solutions. For linear elastic systems, a time step not exceeding 1/10 of the structural period is a good rule of thumb to ensure reasonably accurate numerical results (Chopra, 1995). Theoretical limits on the time step required for stability of the solution have not been determined for nonlinear systems. Changes in stiffness during the response of nonlinear systems may result in equilibrium violations, which ideally must be accounted for to prevent deviation from the correct solution. USEE implements a variable time step algorithm to ensure accuracy and stability, using methods discussed in sections 2.1.2.2 and 2.1.2.3. Additional information on numerical solution methods is available in Clough and Penzien (1993) and Chopra (1995).

2.1.3.2 Time Step Selection

The previous discussion indicated that the size of the time step may affect the stability and accuracy of the numerical computation, and may contribute to equilibrium errors.

Equilibrium errors may result from large changes in stiffness within a step, and therefore are reduced when smaller time steps are used. Reducing the time step increases number of calculations, which increases the solution time and the volume of data generated in the solution. An ideal time step would be sufficiently small to maintain stability and accuracy in the numerical results while not requiring excessive solution times and not producing needlessly large quantities of data.

The size of the ideal time step cannot be identified *a priori*. Instead, computations are done to iteratively refine the time step, either increasing it or decreasing it, as conditions warrant. By using smaller time steps at critical points and larger time steps elsewhere, the number of calculation steps can be reduced while maintaining a specified level of accuracy.

In USEE, as well as in NONSPEC (Mahin and Lin, 1993), the time step (Δt) is selected at the beginning of the time step, based on the following three criteria:

- Δt does not exceed the user-specified time step, $\Delta \tau$.
- Δt does not exceed the time required to reach the next point at which the input acceleration is specified in the base input motion.
- Δt is adjusted (smaller or larger) to satisfy the specified convergence tolerance when the stiffness changes within the time step or a previous step.

The first two criteria for selecting the time step are checked before the step begins; the last criterion is checked at the end of the step.

The last criterion concerns the convergence of the results when stiffness changes during the time step. Figure 3 shows instances where the computed responses "overshoot" the bilinear load-deformation model, when the stiffness changes.

The solid lines in Figures 3(a) and 3(b) represent the paths followed by the computed responses when convergence tolerances are met. The dashed lines represent the correct paths the responses should have taken. To prevent excessive "overshoot" error, the user can specify the convergence tolerance as a percentage of the yield displacement, u_y , in USEE. Overshooting also modifies the shape of the hysteretic curves, as seen in Figure 3(b).

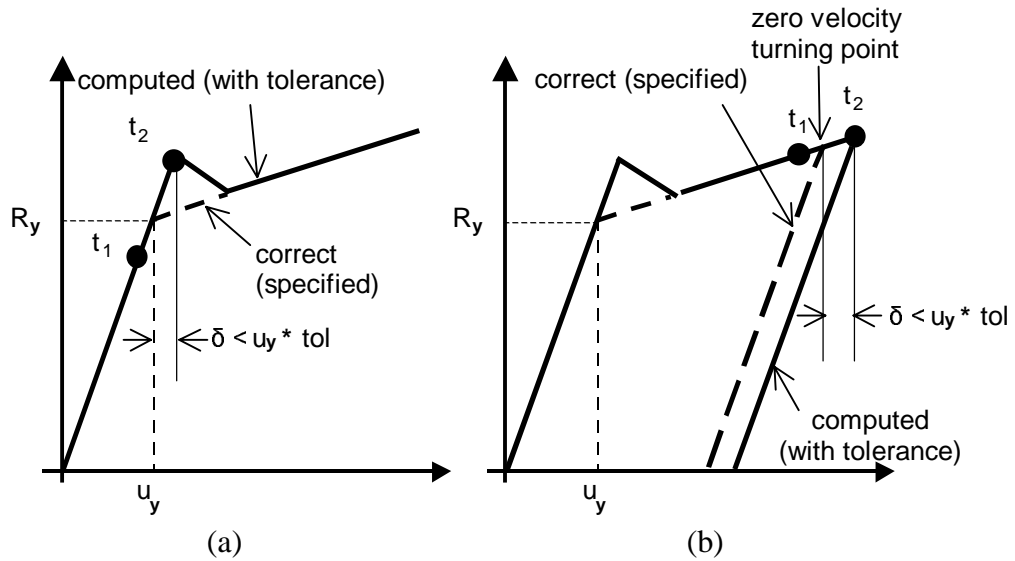


Figure 3. Effect of convergence tolerance on (a) overshoot during loading and (b) hysteretic response on unloading. In the figure, u_y = the yield displacement and tol = the convergence tolerance

The convergence tolerance is checked any time that the stiffness changes. The convergence tolerance is considered to be satisfied in each case if the displacement at the end of a step during which a change in stiffness occurs does not differ by more than the user-specified overshoot tolerance (percentage of u_y) from the displacement at which the change in stiffness occurs. (The displacement difference is shown as δ in Figure 3a and 3b). The correct stiffness (at time $t + \Delta t$) is then used to begin the subsequent time step.

If the convergence tolerance is not satisfied, then the solution for the step is discarded and USEE repeats the calculation beginning at time t with a smaller time increment. The new time step is internally set in USEE to 1/10 of the previous time step. With such a large reduction in the time step, subsequent time steps may not encounter a stiffness change. For this reason, the reduced time step is used for all subsequent steps until a change in stiffness is encountered. If the convergence tolerance is satisfied for the reduced time step, the program continues but reverts to the original time step for subsequent calculations. If convergence is not obtained with the reduced time step, the solution for the last step (using the reduced time step) is discarded and a new time step equal to 1/10 of the previous time step (i.e., one hundredth of the original) is used. This process is repeated until the tolerances are satisfied. However, if the time step is reduced

5 times (to 1×10^{-5} of the original time step) and satisfactory convergence is not obtained, the program stops and notifies the user of the failure to converge.

2.2 Single-Degree-of-Freedom Analogies of Multistory Buildings

Many research studies (e.g. Saiidi and Sozen (1981), Fajfar and Fischinger (1988), Qi and Moehle (1991), Miranda (1991), and Lawson et al. (1994)) have shown that the displacement response of multi-degree-of-freedom (MDOF) buildings often may be approximated by a single-degree-of-freedom (SDOF) system when response is predominantly in a single mode. The SDOF analogue is often termed an “equivalent” SDOF system. Various “equivalent” systems have been described in the literature, but in some cases these systems differ from one another and hence do not represent the concept of equivalency. For this reason, such systems are referred to as SDOF analogues herein. SDOF analogues are used to estimate displacement response in the Nonlinear Static Procedures (NSPs) of ATC-40 (1996) and FEMA-273/274 (1997). Methods for estimating the response of the nonlinear system include the Displacement Coefficient Method, the Capacity Spectrum Method, Yield Point Spectra, and direct computation of the response to a ground motion using software such as USEE. Of the various recommendations for determining the “equivalent” SDOF system, USEE allows the ATC-40 formulation to be used or an alternative formulation that matches the period of the SDOF analogue to the fundamental period of the building. The vertical distribution of mass, a deflected shape (often estimated or assumed equal to the first mode shape), the lateral strength of the building, and either the fundamental period of vibration of the building or the roof displacement that corresponds approximately to yielding of the system are needed to establish the properties of the SDOF analogue. The lateral strength and yield displacement are those that would be observed in a nonlinear static (pushover) analysis of the building when lateral forces are imposed consistent with the assumed mode shape and mass distribution. The USEE implementation assumes that the building may be modeled as a planar structure responding laterally with mass lumped at each floor level. Second order (P-delta) effects and multiaxial excitations (transverse and vertical) response are not explicitly considered.

2.2.1 The “Equivalent” Single-Degree-of-Freedom System

The SDOF analogy relies on the assumptions that the response of the multistory

building is predominantly in a single “mode” and that the deflected shape is proportional to this mode shape throughout the response history. The mode shape used in the analogy need not be identical to the elastic mode shape determined by traditional structural dynamics. Various techniques for establishing an “equivalent” SDOF system have been recommended. Generally, a shape similar to the one that represents the displacement profile of the building at or near its peak response is adequate. Calculated responses usually are not very sensitive to the precise shape selected, and reasonable assumptions often lead to acceptable results.

The equation of motion of a multistory building may be expressed in terms of the degrees of freedom representing the lateral displacements at the floor levels relative to the ground. The equation of motion for such a system is

$$\mathbf{M}\ddot{\mathbf{u}}(t) + \mathbf{C}\dot{\mathbf{u}}(t) + \mathbf{Q}(t) = \mathbf{M}\mathbf{1}\ddot{u}_g(t) \quad (17)$$

where terms are defined conventionally, with \mathbf{M} = diagonal matrix representing lumped masses at the floors of the building, \mathbf{C} = damping matrix of the building system, $\mathbf{Q}(t)$ = vector of story forces at the floor levels, $\mathbf{u}(t)$ = vector of relative displacements at the floor levels, and $\ddot{\mathbf{u}}(t)$ = vector of lateral accelerations of the floors relative to the base of the structure.

A shape vector, ϕ_i , is assumed to represent the deflected shape of the MDOF system throughout its response history. Displacements of the multistory building are tracked at a point known as the “control node.” Many formulations locate the control node at the roof of the building and normalize the shape vector, ϕ_i , to have unit amplitude at the roof. Following this approach, the relative displacement vector may be expressed as the product of the shape vector and the roof displacement, $u_{roof}(t)$, as

$$\mathbf{u}(t) = \phi_i u_{roof}(t) \quad (18)$$

Substituting Eq. 18 in Eq. 17 gives

$$\mathbf{M}\phi_i \ddot{u}_{roof} + \mathbf{C}\phi_i \dot{u}_{roof} + \mathbf{Q} = -\mathbf{M}\mathbf{1}\ddot{u}_g \quad (19)$$

The displacement of the SDOF analogue, u^* , is defined as

$$u^*(t) = \frac{\phi_i^T \mathbf{M} \phi_i}{\phi_i^T \mathbf{M} \mathbf{1}} u_{roof}(t) \quad (20)$$

Pre-multiplying Eq. 19 by ϕ_i^T and substituting for $u_{roof}(t)$ using Eq. 20 results in the following differential equation for the “equivalent” SDOF system:

$$M^* \ddot{u}^*(t) + C^* \dot{u}^*(t) + Q^*(t) = -M^* \ddot{u}_g(t) \quad (21)$$

where:

$$M^* = \phi_i^T \mathbf{M} \mathbf{1} \quad (22a)$$

$$C^* = \phi_i^T \mathbf{C} \phi_i \Gamma_i \quad (22b)$$

$$Q^*(t) = \phi_i^T \mathbf{Q}(t) \quad (22c)$$

$$\Gamma_i = \frac{\phi_i^T \mathbf{M} \mathbf{1}}{\phi_i^T \mathbf{M} \phi_i} \quad (22d)$$

The term Γ_i is also known as the modal participation factor for the i^{th} mode. The value of Γ_i calculated using Eq. 22d depends on how the shape vector is normalized—in this presentation ϕ_i is normalized to have unit amplitude at the roof level. The quantity $\Gamma_i M^*$ is the mass that “participates” in the response associated with $\mathbf{u}(t) = \phi_i u_{roof}(t)$. The mass participation factor, α_i , is the ratio of the participating mass, $\Gamma_i M^*$, to the total mass:

$$\alpha_i = \frac{\phi_i^T \mathbf{M} \mathbf{1}}{\phi_i^T \mathbf{M} \phi_i} \frac{\phi_i^T \mathbf{M} \mathbf{1}}{\mathbf{1}^T \mathbf{M} \mathbf{1}} \quad (23)$$

The value of the mass participation factor, α_i , is independent of the manner in which the shape vector is normalized.

The load-deformation relation of the SDOF analogue usually is determined from the capacity curve obtained from a nonlinear static (pushover) analysis of the structure. The capacity curve plots the base shear force versus roof displacement of the structure. Figure 4 shows an idealized capacity curve that was obtained by applying lateral forces proportional to the product of amplitude of the shape vector and mass at each floor level. A bilinear curve was fit to the capacity curve for use in determining the load-displacement relation of the SDOF analogue.

Eq. 20 may be restated to more concisely express the relation between the yield displacement of the SDOF analogue and the yield displacement of the multistory system as:

$$u_y^* = \frac{u_{roof,y}}{\Gamma_i} \quad (24)$$

Different approaches have been recommended for relating the base shear strength of the multistory system to the yield strength of the SDOF analogue. USEE allows the user to select from two implementations that are described generally by Figure 4(b). These implementations are defined as follows:

The bilinear curve fit to the capacity curve represents a case when yielding occurs at a sharply defined point. The vector of lateral forces at the instant of yielding, \mathbf{F}_y , can be expressed as

$$\mathbf{F}_y = \mathbf{K}\mathbf{u}_y = \mathbf{K}\phi_i u_{roof,y} \quad (25)$$

The yield strength of the multistory building observed in the pushover analysis, also known as the base shear strength at yield, is the sum of the story forces

$$V_y = \mathbf{1}^T \mathbf{F}_y \quad (26)$$

The base shear coefficient at yield is given by

$$C_y = \frac{V_y}{W} = \frac{\mathbf{1}^T \mathbf{K} \phi_i u_{roof,y}}{\mathbf{1}^T \mathbf{M} \mathbf{1} g} \quad (27)$$

Orthogonality relations (Clough and Penzien (1993), Eq. 11-39) provide that

$$\mathbf{1}^T \mathbf{K} \phi_i = \omega_i^2 \mathbf{1}^T \mathbf{M} \phi_i \quad (28)$$

if ϕ_i is an elastic mode shape, with ω_i = the circular frequency associated with vibration in the i^{th} mode. Substituting Eqs. 28 and 24 into Eq. 27 results in

$$C_y = \omega_i^2 \frac{\mathbf{1}^T \mathbf{M} \phi_i}{\mathbf{1}^T \mathbf{M} \mathbf{1}} \frac{\Gamma_i u_y^*}{g} = \frac{\omega_i^2 \alpha_i u_y^*}{g} \quad (29)$$

The yield strength of the SDOF analogue, F_y^* , can be expressed as:

$$F_y^* = K^* u_y^* = \omega^{*2} M^* u_y^* \quad (30)$$

Hence, the yield strength coefficient of the SDOF oscillator is

$$C_y^* = \frac{F_y^*}{M^* g} = \frac{\omega^{*2}}{g} u_y^* \quad (31)$$

To cause the SDOF analogue to have a natural period of vibration that matches the i^{th} period of vibration of the MDOF system, the circular frequency ω^* should be set equal to

the i^{th} circular frequency, ω_i^* . Doing so results in

$$C_y^* = \frac{\omega_i^2}{g} u_y^* = \left(\frac{2\pi}{T_i} \right)^2 \frac{u_y^*}{g} \quad (32)$$

where $T_i =$ the natural period of vibration of the i^{th} mode. This implementation (Eq. 32) assures that the natural period of the SDOF analogue matches a natural period of vibration of the MDOF system regardless of whether the shape vector corresponds to an elastic mode or not.

The ATC-40 implementation uses Eqs. 29 and 32 to express C_y^* as

$$C_y^* = \frac{C_y}{\alpha_i} \quad (33)$$

The yield strength of the SDOF analogue is given by $V_y^* = C_y^* W^* = V_y / \Gamma_i$, representing the notion that the yield strength coefficient associated with the mass that participates in the i^{th} mode can be related to a smaller yield strength coefficient (C_y) that is associated with the total mass of the structure. Eq. 33 is used to determine the strength of the SDOF analogue in ATC-40 and represents one of the implementations available in USEE.

Any shape vector ϕ_i may be specified in USEE. If an elastic mode shape is used for ϕ_i , then the natural period of vibration of the SDOF analogue will match the period of vibration of the multi-degree-of-freedom system, whether computed using Eq. 32 or Eq. 33. If the shape vector is not identical to an elastic mode shape, then the period of the SDOF analogue obtained in the ATC-40 implementation (Eq. 33) will not match the corresponding period of vibration of the multistory system, while Eq. 32 assures that the period of vibration of the “equivalent” SDOF matches a period of the multi-degree-of-freedom. Both implementations are available in USEE.

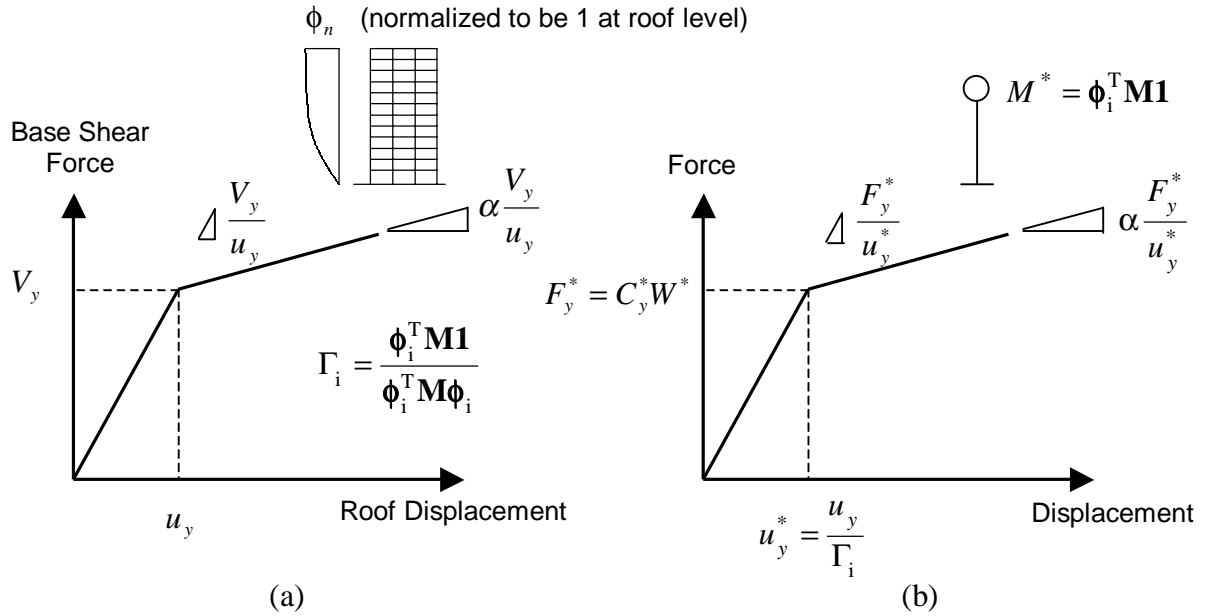


Figure 4. Establishing the properties of an “equivalent” SDOF system: (a) capacity curve determined from the nonlinear static (pushover) analysis of the building, (b) load-deformation curve of the SDOF analogue, derived from the capacity curve

2.2.2 Implementation of the SDOF Analogue in USEE

The *Multistory Building Approximation* analysis module within USEE provides a simple means to estimate the displacement response of a multistory building based on a SDOF analogue.

The user specifies the distribution of floor mass over the height of the building, story heights, and the deflected shape to be used in making the analogy. For many buildings, the distribution of mass is nearly uniform, resulting in M^* and Γ_i being dependent only on the deflected shape. The user may specify arbitrary deflected shapes, or one of the three deflected shapes suggested by Abrams (1985) may be selected (Figure 5). As an initial approximation, the parabolic shear deflected shape may be suitable for many regular moment-resistant frame buildings, and the flexure beam deflected shape may be suitable for many structural (shear) wall buildings. For many buildings, the precise shape is not necessary to obtain good estimates of peak displacement response, and one or two of these shapes may be used to determine approximate values or ranges of expected peak displacement response.

The user indicates the yield strength that would be observed in a nonlinear static (pushover) analysis of the building via the base shear coefficient, C_y . The period of vibration of the building or the yield displacement is needed to establish the elastic portion of the load-deformation curve. Either may be specified.

The yield strength coefficient, C_y^* , of the SDOF analogue can be established by two alternative approaches, as described in Section 2.2.2. Eq. 32 assures the period of vibration of the SDOF analogue matches the period specified for the multistory building. The ATC-40 implementation (Eq. 33) gives identical results provided that the elastic mode shape is used for the shape vector.

The user is cautioned to validate results by other means where assumptions may be in question or when the consequences are significant.

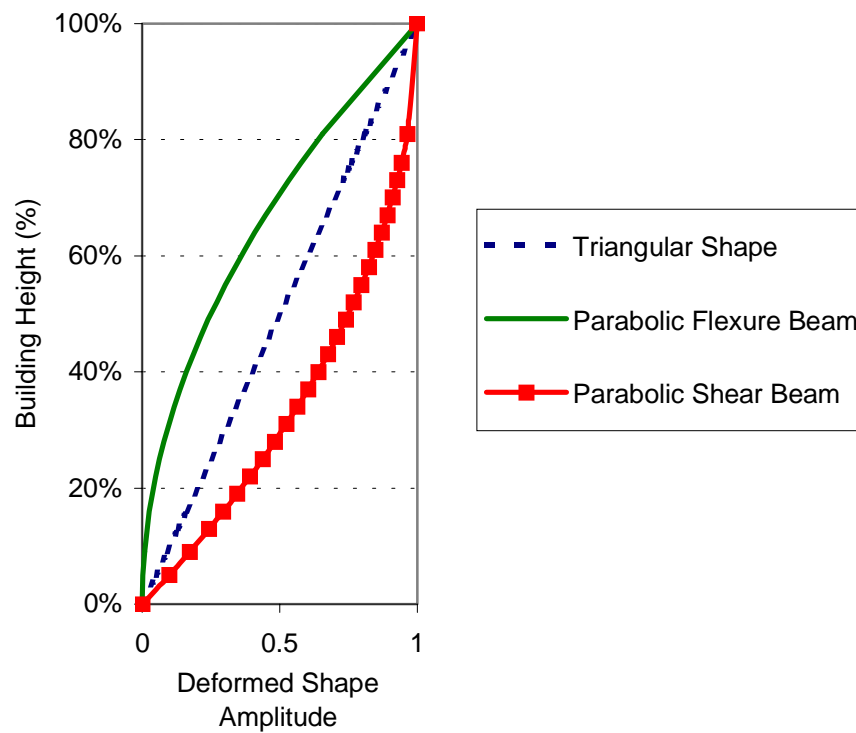


Figure 5. Default mode shapes available in USEE

2.3 Computation of Response Spectra Using USEE

USEE provides robust tools for computing various types of response spectra for both linear elastic and nonlinear response. The spectra plot the peak response values that occur

over the duration of shaking for a specified range of vibration periods. Computed results may be plotted as a function of period or the yield or peak displacement of the oscillator, providing various representations of the underlying data. Elastic spectra, constant strength spectra, constant strength reduction factor spectra, and constant ductility spectra may be computed, using the linear, bilinear, and stiffness-degrading load-deformation models for any of the base input accelerations available for the SDOF analysis. Details of the computation of response spectra in USEE and the required parameters are described in the following sections.

2.3.1 Specification of Periods

The range of periods used in the computation of response spectra is specified by the user. Either of two distributions of periods within this range may be selected: a uniform distribution or a geometric distribution. The geometric distribution provides a denser spacing of periods at the lower end of the period range, where response often has greater variation. The geometric ratio, r , of a set of N periods is given by:

$$r = \exp\left\{\frac{\ln(T_N) - \ln(T_1)}{N - 1}\right\} \quad (34)$$

where

$$T_i = r^{i-1}T_1 \quad (35)$$

and T_1 = lower period, T_N = upper period, T_i = an intermediate period, and N = number of periods.

2.3.2 Computation of Elastic Response Spectra

The peak response of linear elastic SDOF oscillators subjected to a specified input motion is conveniently described by the elastic response spectrum. For each oscillator, the peak displacement of the mass relative to the base (the peak relative displacement, often called the peak displacement or peak deformation), S_d , is computed for the user-specified periods of vibration and viscous damping. The pseudo-acceleration, S_a is computed as

$$S_a = \omega^2 S_d \quad (36)$$

where ω = circular frequency of vibration = $2\pi/T$.

The response spectrum module in USEE guides the user through three data input screens. The following actions are required to compute the elastic response spectra:

1. The user selects the input excitation.
2. The user selects the linear-elastic load-deformation model.
3. The user specifies the range of periods, number of periods, and whether a uniform or geometric distribution of periods is desired.
4. The user specifies the viscous damping ratio as a percentage of critical damping. Up to 5 damping ratios may be specified in each computation of elastic response spectra.

USEE calculates the response histories using the numerical method described in Section 2.1 and determines the peak relative displacement and spectral acceleration, S_a , for the specified values of period and damping. Peak relative displacement or pseudo-acceleration may be plotted against period for each value of damping.

2.3.3 Computation of Inelastic Response Spectra

Inelastic response spectra provide a convenient means to summarize the peak responses of nonlinear SDOF oscillators subjected to a specified base input motion. Three types of inelastic response spectra may be computed in USEE: constant strength spectra, constant strength reduction factor (R-factor) spectra, and constant ductility spectra. Each type of spectra may be computed using the bilinear or stiffness-degrading load-deformation model. The excitation, load-deformation model, damping and post-yield stiffness values are kept constant in any computation. The user specifies a period range and up to 5 values of the strength, R-factor, or ductility for which the spectra are to be computed. Spectral response quantities (yield strength coefficient, peak strength normalized by weight, peak relative displacement, peak ductility, and absolute acceleration normalized by the acceleration of gravity, g) may be plotted versus period of vibration, yield displacement, or peak relative displacement. The type of response spectrum, the number of periods, and the number of parameters for which the response spectra are to be computed affects the time required for computation. In particular, computation of constant ductility spectra is an iterative process that requires substantially more time to compute.

To compute inelastic response spectra, the following actions are required of the user:

1. The user selects a base input acceleration.

2. The user selects a load-deformation model (bilinear or stiffness-degrading).
3. The user specifies a period range and the number of periods, as well as the distribution of periods.
4. The user specifies a viscous damping ratio (as a percentage of critical damping).
5. The user specifies a post-yield stiffness as a percentage of initial stiffness.
6. The user specifies the parameter to be varied in the inelastic response spectra computation, as well as specific values of this parameter.

USEE calculates the response histories for the specified periods and parameter values using the numerical method described in Section 2.3.1. Appendix B describes the iterative algorithm used for computing isoductile spectra. Peak response quantities are retained for each case (yield strength coefficient, peak ductility, and R-factor). These quantities may then be plotted as a function of period, yield displacement, or peak relative displacement.

2.3.3.1 Constant Strength Spectra

Constant strength spectra refer to the response of oscillators having constant yield strength. The excitation, load-deformation model, damping, and post-yield stiffness are kept constant over a range of periods. Up to 5 values of the yield strength coefficient may be specified. The peak relative displacement and the peak ductility responses are often of interest. However, other response quantities may also be plotted in the *View Results* window.

2.3.3.2 Constant Strength Reduction Factor (R-Factor) Spectra

Constant R-factor spectra may be of interest when constant strength reduction factors are used for determining the strength of SDOF oscillators. Inelastic response spectra are computed for user-specified R-factors for the specified excitation, load-deformation model, damping and post-yield stiffness. To determine the strengths of the oscillators, USEE first computes the elastic response spectrum over the specified vibration periods. Yield strength coefficients are calculated for each period and R-factor as

$$C_y = \frac{S_a/g}{R} \quad (37)$$

where C_y = yield strength coefficient, S_a = pseudo-acceleration associated with linear elastic response, g = acceleration of gravity, and R = strength reduction factor.

Peak displacement ductility demands may be viewed in the *View Results* window, along with other parameters including absolute acceleration, yield strength coefficient, and peak relative displacement.

2.3.3.3 Constant Ductility Spectra

For the preceding types of spectra, the response for specified oscillator properties is computed for a specified excitation. In some cases, it is desired to determine oscillator properties so that a given response characteristic is obtained. Constant ductility spectra are computed by iterating on strength to identify the strength required to obtain a ductility response equal to the specified ductility value, for each oscillator. Up to five ductility values may be specified. The excitation, load-deformation model, damping, and post-yield stiffness are kept constant throughout the computation. The yield strength coefficients required to limit ductility demands to the specified values may be displayed in the *View Results* window, along with the response parameters stated above.

The iterative nature of the computation requires significantly more computational time than is required for the other response spectra. The algorithm is described in detail in Appendix B.

The user may change the parameters that control the accuracy and efficiency of the constant ductility computation. These parameters are shown in Table 1 with their corresponding limits and default values. Terms are defined and discussed in more detail in Appendix B.

Table 1. Constant ductility algorithm parameters

		Lower Bound		Default Value	Upper Bound	
		Limit	Advisory		Advisory	Limit
Tolerance on target ductility (as % of target ductility)		0.01	0.1	0.25	10	20
Tolerance on yield strength coefficient (%)		0.01	0.1	0.45	10	20
Initial bounding of solution range	Smoothness tolerance (%)	1	5	30	50	70
	Criteria to switch to fast search					
	Ductility (as % of target ductility)	0	0	90	95	100
	Strength interval (as % of isoductile strength)	0	5	10	100	100

3 User's Manual

3.1 Installing and Maintaining the Program

3.1.1 USEE Distribution

The USEE distribution is compiled for use with the Windows 95/98/2000 and NT4.0 operating systems. USEE is distributed in compact and full versions. The compact version includes with the software a very limited suite of synthetic motions. The full version includes the complete suite of 120 synthetic motions that were generated in the Mid-America Earthquake Center Project RR-1. Both versions include a modest suite of recorded ground motions.

3.1.2 Hardware Recommendations

The compact version requires approximately 16 MB of disk space, depending on whether files common to other applications are already present. The full version requires an additional 25 MB of disk space. A screen resolution of 1024 x 768 is recommended, although an 800 x 600 display resolution is sufficient.

3.1.2.1 Obtaining and Installing the Program

The software may be obtained using any standard internet web browser from the Mid-America Earthquake Center web site (<http://mae.ce.uiuc.edu>). Once downloaded, installation is as simple as double-clicking on the SETUP.EXE file. The installation routine will present a number of dialog boxes. Files will be installed on the user's hard drive. Existing files will not be replaced without the user's explicit consent. If USEE is being installed over a pre-existing installation of USEE, the pre-existing installation should be uninstalled prior to installing the new version.

3.1.3 Un-installation Guide

USEE may be uninstalled using the Windows uninstall feature. In Windows 95/98/2000, and NT4.0, this is accessed from the **Control Panel** under the **Add/Remove Programs** icon. This process will not delete files common to other installed applications.

3.1.4 Maintenance and Support

Support is handled electronically via the Mid-America Earthquake Center web site (<http://mae.ce.uiuc.edu>). This site provides information on:

- The current release of the program
- Comments from users and bug reports

- Release history information

Please feel free to contact the authors to provide your comments, to request new features, and to report bugs (inel@uiuc.edu, ebretz@uiuc.edu, and aschheim@uiuc.edu).

3.2 Program Design

The program utilizes a modular design. Program modules are accessed from the main window by mouse-driven command menus. USEE 2001 provides modules for

- Single-Degree-Of-Freedom (SDOF) analysis
- Multistory Building Approximation analysis (using SDOF analogues)
- Response Spectra computation

Each module is implemented using a “wizard” that guides the user through a series of windows for data entry and viewing of results. Each window is a “step” in the module, and the user may freely navigate forwards and backwards through the data input screens. Each time the **Compute Results** button is clicked, a run number is assigned to the analysis. This run number is unique in any analysis session.

3.2.1 Module Operation

Each module provides a series of windows for data input and viewing of results. Base input motions and load-deformation models are selected in designated windows in each analysis module. The *Multistory Building Approximation* analysis module has an additional input window for specifying floor masses, story heights, and the assumed mode shape. Results for all three analysis modules are viewed in a *View Results* window.

Each step in the sequence provides guidance to the user. USEE *Help* may be accessed by selecting **Help** from the menu bar. The **Save As Default** button in each window adopts the values in the current window as default values for subsequent analyses. The **Compute Results** button uses current input values for the computation and advances directly to the **View Results** window. The main window provides menu choices for beginning a new analysis, opening an existing file, saving current analysis files, and exporting the results of the current analysis to ASCII text files, for subsequent processing by the user. Only the input data is saved in an analysis file.

3.2.2 Directory Structure

The USEE program is installed to **C:/Program Files/USEE** unless otherwise specified by the user during the installation. Beneath the top level directory where USEE

is installed are four subdirectories: **Help**, **Multistory**, **Response_Spectra**, **SDOF**, and **Waveforms**. The complete USEE subdirectory structure is

USEE/
USEE/Help/
USEE/Multistory/
USEE/Response_Spectra/
USEE/SDOF/
USEE/Waveforms/
USEE/Waveforms/Recorded/
USEE/Waveforms/Synthetic/
USEE/Waveforms/Synthetic/Hard Rock
USEE/Waveforms/Synthetic/Soil

The subdirectories titled **Multistory**, **Response_Spectra**, and **SDOF** contain input data for the analyses that were previously saved by the user. The **Help** folder contains files necessary for the help menus. The **Waveforms** subdirectory contains individual files for each synthetic and recorded ground motion made available in USEE. If the user wishes to use a ground motion record not supplied with USEE, the file should be placed in the recorded waveforms subdirectory. Formatting requirements for user-supplied accelerograms are described in Section 3.5.1.2. The synthetic ground motion files are distributed into separate subdirectories based on the soil type.

3.3 Using the Program

3.3.1 Description of Commands

Command buttons and toolbar commands are as follows:

Back: takes the user back to the previous step in an analysis module.

Compare Results: takes the user to the *Compare Results* window. This requires the current analysis to be saved, raising a dialog box if needed.

Compute Results: computes results with user specified input data and advances to the *View Results* window. Default values are used for any steps omitted by the user.

Copy: copies the selected plot as a bitmap image to the Windows clipboard.

Export Output: saves the current analysis output as an ASCII text file under a user-specified file name.

Exit SDOF Oscillator Session: exits the current SDOF Oscillator analysis session, closing all windows except the main USEE window.

Exit Multistory Building Approximation Session: exits the current Multistory

Building Approximation analysis session, closing all windows except the main USEE window.

Exit Response Spectra Session: exits the current Response Spectra analysis session, closing all windows except the main USEE window.

Exit USEE: exits the program, closing all windows.

Load Existing File: loads an existing file of the current analysis type (*Single-Degree-of-Freedom, Approximate Multistory Building, and Response Spectra*). The existing file is opened, input values are loaded, response is computed, and results are displayed in the *Compare Results* window. This is a shortcut to facilitate comparing responses from multiple analyses.

New: creates a new analysis file having an extension appropriate for the current analysis type (e.g. NEW1.SDOF, NEW1.BLDG, OR NEW1.RSPC).

Next: takes the user to the next step in an analysis module.

Open: locates and opens a previously saved analysis file; the file name extension is appropriate to the current analysis type.

Refresh Plots: refreshes plots in the *View Results* window. This is needed whenever the user changes a plotting parameter, such as color, time interval, or number of plots.

Return To Results Window: closes the current window and returns to *View Results* window.

Save: saves the current analysis file.

Save As: saves the current analysis file under a user-provided file name.

Save As Default: saves the current window data as default values for use in subsequent analysis sessions.

Show Constant Period Line: draws a constant period line on the plot in the *View Results* step a *Response Spectra* analysis if the capacity spectra (peak strength / weight vs. peak relative displacement) or yield point spectra (yield strength coefficient vs. yield displacement) is active.

Start New Analysis: creates a new analysis having an extension appropriate for the current analysis type (.SDOF, .BLDG, .RSPC).

Test Model: allows the selected load-deformation model to be exercised manually by incrementing displacements step by step.

View Accelerogram: plots the accelerogram of the selected input motion, whether recorded or synthetic.

View File Header: displays header information from the selected input motion, whether recorded or synthetic.

View Summary Log: views summary log file for the current analysis session

Visit Mid-America Earthquake Center Homepage: loads the Mid-America Earthquake Center Homepage using a previously-installed web browser.

Zoom To Full Screen: zooms in on results plot.

F1 function key: brings main window for USEE *Help*. The user can go to the main help window from any step of the USEE program by pressing the **F1** key function.

3.3.2 User Preferences

Units, values of parameters used in the computations, and export options may be set from the **Preferences** menu at any time.

3.3.2.1 Available Units

USEE uses either in U.S. Customary or SI units to display and input data. The units to be used may be specified from the **Preferences** menu or the **Units** pull-down list box on the toolbar at the top of the screen.

Available force units are as follows:

- U.S. Customary: pounds (lb) or kips (kips).
- International System (SI): Newtons (N) or kiloNewtons (kN).

Available length units are as follows:

- U.S. Customary: inches (in), or feet (ft).
- International System (SI): centimeters (cm), or meters (m).

The units used to display data may be changed at any time; internal computations are done in kN and cm units.

3.3.2.2 Parameters

Parameters that the user can set are computational time step, output time step, and overshoot tolerance.

The ideal time step value cannot be identified *a priori*. The smaller of the user-specified time step and the time required to reach the next acceleration point of the base input is used at the beginning of each step. Typically, a value not exceeding 10% of the

period would be specified by the user. The program will automatically reduce the time step if required for convergence of the solution (Section 2.1.2.2).

USEE can report response data according to the user-specified output time step. A large number of time steps may be needed to ensure accuracy of the solution. This has the potential to generate a large amount of data. If the user prefers, data may be output less frequently without changing the size of the time step used in the computations. The output time step is specified as an integer multiple of the computation time step. The user may choose the output to be reported at 1, 2, 5, or 10 times the user-specified time step. Values of 2 or more cause corresponding reductions in the size of the data files.

The overshoot tolerance is used to check convergence for the nonlinear response any time that the stiffness changes. It is specified as percentage of the yield displacement. The convergence is considered to be satisfied in each case if the displacement at the end of a step during which a change in stiffness occurs does not differ by more than the user-specified overshoot tolerance (percentage of u_y) from the displacement at which the change in stiffness occurs (Section 2.1.2.2).

Parameters that control the constant ductility iterations are described in Appendix B.

3.3.2.3 Export Options

The user can manage the size of the exported output by choosing what to report from the provided checkbox list that includes displacement, absolute velocity, absolute acceleration, force, and energy related parameters.

3.3.3 SDOF Analysis Steps

The “wizard” interface for SDOF analysis presents the user with three windows in sequence; the first two provide for data input and the third displays response quantities and plots. The following actions are required.

Step 1: Select the appropriate tab to choose base input: recorded ground motions, synthetic motions, or simple pulses.

Step 2: Select a load-deformation model and specify values of model parameters.

Step 3: View response plots and summary statistics.

Quantities to be displayed on the plot are selected from the pull down list boxes located on each plot axis. The **Zoom to Full Screen** button provides greater detail. With the cursor located over any plot, a right click of the mouse or clicking the toolbar **Copy**

button copies the plot to the Windows clipboard. The plot can now be pasted into other Windows applications such as Microsoft Word. Analysis results may be exported to formatted ASCII files by clicking on the **Export Output** button. Results may be compared to previously completed analyses in the *Compare Results* window, accessible from this step. The input files for the previous analyses must have been saved previously.

3.3.4 Multistory Building Approximation Analysis Steps

The displacement response of buildings that respond predominately in a single mode may be determined approximately using an analogous SDOF oscillator. The oscillator characteristics may be established using the procedure described in Section 2.2.1 of this report. The drift profile (shape vector) story heights, and mass distribution are specified in the first input window of this module; three subsequent windows characterize the base input, load-deformation response, and computed response data.

Step 1: Specify number of stories, story heights, mass (or weight) distribution, and mode shape.

Step 2: Select the appropriate tab to choose recorded ground motions, synthetic motions, or simple pulses for base input acceleration.

Step 3: Select load-deformation model and specify parameter values to define the base shear versus roof displacement relation.

Step 4: View response plots and summary statistics.

Pull down list boxes allow various quantities to be plotted in the *View Results* window.

3.3.5 Response Spectra Analysis Steps

This module provides three windows; two provide for data input and the third displays response data and plots:

Step 1: Select the appropriate tab to choose recorded ground motions, synthetic motions, or simple pulses for base input acceleration.

Step 2: Select a load-deformation model and specify response spectra parameters.

Parameters that may be varied include viscous damping, yield strength coefficient, strength reduction factors, and displacement ductilities. The last case requires an iterative solution to determine oscillator strengths, and is more time consuming.

Step 3: View summary statistics and response plots.

Pull down list boxes allow the user to select quantities to be plotted. The selection set depends on the type of response spectra that were computed. Quantities may be plotted versus period, the peak relative displacement, or yield displacement. When constant ductility or constant strength reduction factor (R-factor) spectra are computed, Yield Point Spectra may be displayed by plotting yield strength coefficient versus yield displacement. Alternatively, constant ductility or constant strength reduction factor spectra may be displayed in a Peak Capacity Spectrum Method format by plotting peak strength coefficient versus peak displacement. When Yield Point Spectra or peak spectra are plotted, the cursor can be positioned on screen to provide a schematic illustration of the yield and peak points for any computed period.

While in any of the analysis modules, the user may move backward and forward to different windows (steps), modify input parameters, and then advance to last step to view the results. Advancing to the last step in the *Response Spectra* module causes the spectra to be recomputed using the modified values. This may be time-consuming if numerous calculations are required, particularly in the case of constant ductility spectra.

3.3.6 Windows Copy & Paste

Response plots may be copied to Windows applications such as Microsoft Word using the **Copy** and **Paste** functions. These may be accessed via the toolbar or a right mouse click. To copy a response plot, first left click on the plot to select it and then select **Copy** from the toolbar, or simply right click on the plot and select **Copy** on the submenu. Then switch to another application (such as Microsoft Word) and select **Paste** from the menu bar.

3.3.7 Input and Output Data Files

Individual analysis data input files can be saved for subsequent recall and for use in the *Compare Results* step. The filenames are saved with the following extensions: *.SDOF* for *SDOF* analyses, *.BLDG* for *Multistory Building Approximation* analyses, and *.RSPC* for *Response Spectra* analyses. These extensions are automatically supplied if not specified by the user. The files are binary.

Input parameters and output summaries may be saved as ASCII text when viewing response data. Complete data files will be created and saved as ASCII text by clicking the **Export Output As** menu item when viewing response data. Output files are saved with

.TXT extensions.

The quantities available for export are shown in Table 2:

Table 2. Response quantities available for export

<i>Single-Degree-of-Freedom</i>	<i>Multistory Building Approximation</i>	<i>Response Spectra</i>
Displacement	Roof Displacement	Period
Absolute Velocity	Absolute Roof Velocity	Yield Displacement
Absolute Acceleration	Absolute Roof Acceleration	Damping
Force / Weight	Force / Weight	Post-Yield Stiffness
Elastic Strain Energy / Weight	Elastic Strain Energy / Weight	Ductility
Input Energy / Weight	Input Energy / Weight	Yield Strength Coefficient
Kinetic Energy / Weight	Kinetic Energy / Weight	Peak Displacement
Damping Energy / Weight	Damping Energy / Weight	Total Acceleration
Hysteretic Energy / Weight	Hysteretic Energy / Weight	Peak Strength / Weight

Graphs that plot results may be copied and pasted to other Windows applications using the right mouse key.

3.3.8 Summary Data Files

A summary of numerical results from the current analysis session is provided to the user. Each analysis run during the session is listed. At the top, the date and time is provided, followed by the properties specified by the user, and calculated quantities and peak response values.

3.4 Modeling and Response Computation

3.4.1 Load-Deformation Models

USEE features three commonly used load-deformation models: linear elastic, bilinear, and stiffness degrading. These are described in this section.

3.4.1.1 Linear Elastic Model

The linear elastic model (Figure 6) is used in most introductory courses in structural dynamics and is applicable to the response of structures that remain elastic, such as for relatively small ground shaking intensities. For linear elastic response, only the stiffness is needed to characterize the load-deformation curve.

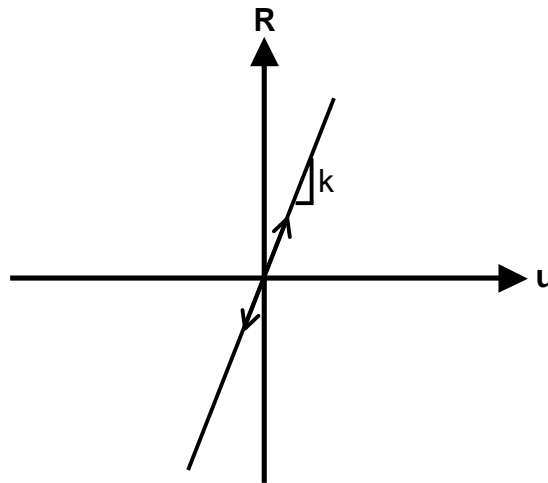


Figure 6. Linear elastic model

3.4.1.2 Bilinear Model

Bilinear models are applicable to structures that exhibit stable and “full” hysteretic loops, and often are used for modeling steel structures. The bilinear model (Figure 7) is defined by three parameters: yield strength, initial stiffness, and post-yield stiffness. Strength is bounded by the yield envelope curves. Unloading from the curves occurs with stiffness equal to the initial (elastic) stiffness. The elastic-perfectly plastic model is a special case obtained by specifying post-yield stiffness to be zero.

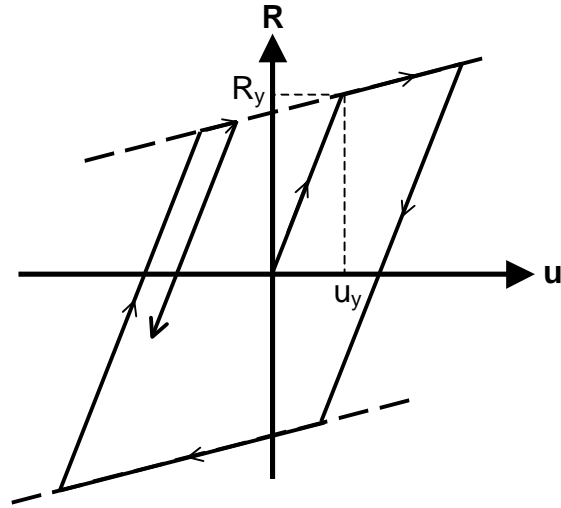


Figure 7. Bilinear model

3.4.1.3 Stiffness-Degrading Model

Various stiffness-degrading models have been used to represent reinforced concrete structures. The stiffness-degrading model implemented in USEE is suitable for structures that do not exhibit substantial degradation due to shear or bond deterioration, which can cause severe strength degradation and/or pinching of the hysteretic curves. This model uses a bilinear envelope curve defined by three parameters: the yield strength, the initial stiffness and post-yield stiffness. Figure 8 shows the stiffness degrading characteristics of this model during load reversals. Unloading begins with the initial elastic stiffness; when the load changes sign (crossing the displacement axis), the stiffness changes and the model loads toward the previous peak in the direction of motion. If prior yielding has not occurred in the direction of motion, the model loads toward the yield point.

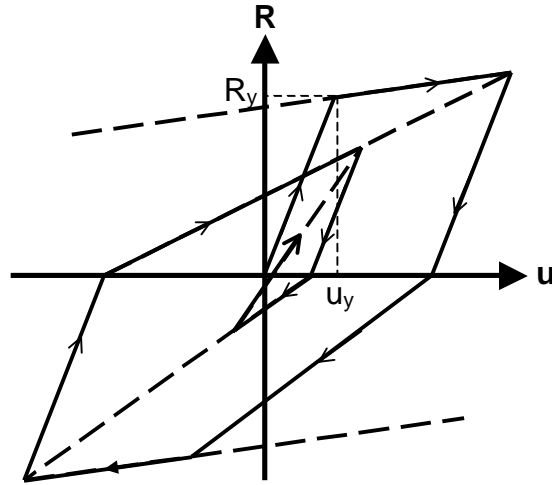


Figure 8. Stiffness-degrading model

3.4.2 Load-Deformation Curve Properties

3.4.2.1 Yield Strength Coefficient, C_y

The yield strength coefficient, C_y , is defined as yield strength of the oscillator divided by its weight.

$$C_y = \frac{F_y}{W} \quad (38)$$

where F_y = yield strength of oscillator and W = weight of oscillator.

3.4.2.2 Base Shear Coefficient, C_y

The base shear coefficient, C_y is defined as the base shear strength at yield divided by the weight of the building:

$$C_y = \frac{V_y}{W} \quad (39)$$

where V_y = base shear strength of the building at yield and W = weight of the building.

3.4.2.3 Period of Vibration

The natural period of vibration, T , of the system is defined as the time required to complete one cycle of free vibration of the system if undamped. This period is related to the circular frequency, ω , by $T= 2\pi/\omega$, where

$$\omega = \sqrt{\frac{K}{M}}$$

and K and M are the stiffness and mass of the SDOF oscillator, respectively. The frequency of vibration, f , is the inverse of the period:

$$f = \frac{1}{T}$$

3.4.2.4 Damping

Viscous damping is specified relative to critical damping, with critical damping defined as

$$c_c = 2M\omega \quad (40)$$

The critical damping ratio, ξ , is specified in the USEE input, defined by

$$\xi = \frac{c}{c_c} = \frac{c}{2M\omega} \quad (41)$$

Values of 2-5% are typical of many common structures.

3.4.2.5 Initial Stiffness

The initial stiffness is the slope of elastic portion of load-deformation response of oscillator. It must be positive.

For *Single-Degree-of-Freedom* analysis, the stiffness may be determined as the ratio of yield strength, F_y and yield displacement u_y :

$$K_1 = \frac{F_y}{u_y} \quad (42)$$

For *Multistory Building Approximation* analysis, the stiffness can be determined from the load-deformation relation of the “equivalent” SDOF system. This stiffness may be derived from the user-specified load-deformation relation of the MDOF system using the formulation given in Section 2.2.1 as:

$$K_1^* = \frac{F_y^*}{u_y^*} \quad (43)$$

3.4.2.6 Post-Yield Stiffness, α

The post-yield stiffness is the slope of the load-deformation curve after yielding of the oscillator. It is specified as a percentage, α , of the initial stiffness:

$$\alpha = \frac{K_2}{K_1} \quad (44)$$

where K_2 is the slope of the load-deformation curve after yielding (Figure 8). Values of α between -100% and 100% may be entered for all analyses except for constant ductility response spectra, for which only non-negative values of α are allowed.

Negative values of post-yield stiffness may result in the collapse of the oscillator (Figure 9(b)). Under static loading, collapse is defined when the restoring force decreases to zero (at Δ_c of Figure 9(b)). At larger displacements, the restoring force changes sign to act in the direction of the displacement, causing the displacement to grow without limit. Under certain dynamic conditions, it is possible for the oscillator to exceed the static collapse displacement and not collapse, provided that accelerations drive the oscillator back towards the origin. USEE is internally set to halt computation if displacements exceed 1.2 times the static collapse displacement. When this occurs, a large dot is plotted at the last completed time step in the View Results window of the SDOF and Multistory Approximation modules. In the Response Spectrum module, no information is plotted for oscillator responses that exceed $1.2\Delta_c$. Each instance that this occurs results in a discontinuity in the response spectrum plots.

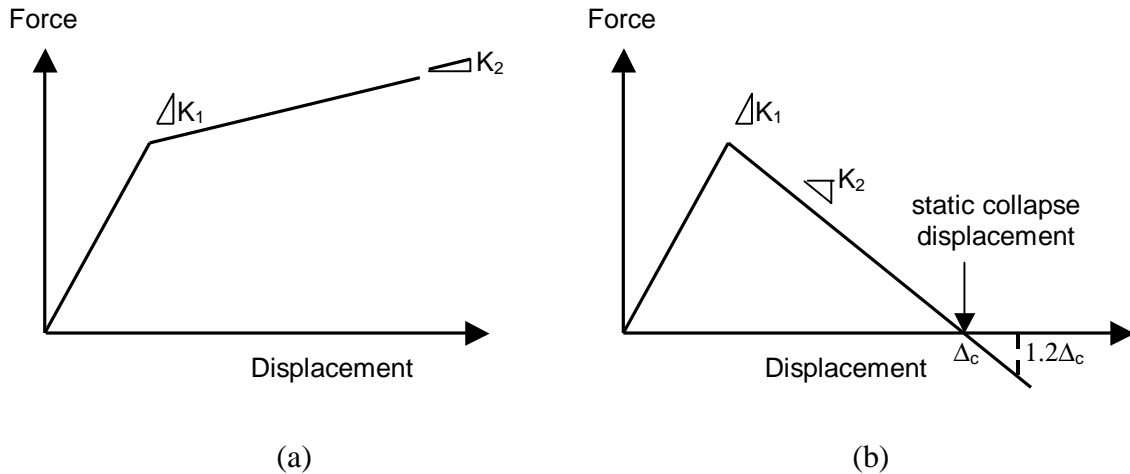


Figure 9. Load-deformation response of a bilinear oscillator with (a) positive post-yield stiffness, (b) negative post-yield stiffness

3.4.2.7 Yield Displacement, Δ_y

The yield displacement is the displacement of the structure relative to the ground at the instant that the structure reaches its yield strength.

3.4.2.8 Building Drift at Yield

The building drift at yield is the roof displacement relative to the base of the structure at the instant when the structure reaches its base shear strength (at yield).

3.4.3 Response Spectra Parameters

See Section 2.3.

3.5 Base Motion Input

The setup program installs a suite of base motions in the subdirectory **USEE\Waveforms**, where **USEE** is the highest level directory for the program specified during the installation. Recorded ground motions are located in the **USEE\Waveforms\Recorded** subdirectory and synthetic motions are located in the **USEE\Waveforms\Synthetic\Hard Rock** and **USEE\Waveforms\Synthetic\Soil** subdirectories.

3.5.1 Recorded Ground Motions

3.5.1.1 Recorded Ground Motion Filenames

Selecting the *Recorded Ground Motions* tab of the base input screen displays all files present in the **USEE\Waveforms\Recorded** subdirectory. There is no restriction on naming base motion input files. The “11.3” filename convention used in the USEE

distribution follows the format, EQYRSTATBRG.EXT

where:

EQ= 2 characters representing the earthquake.

YR= 2 digits representing the year of the earthquake.

STAT= 4 characters representing the name of the recording station

BRG= 3 digits representing the compass bearing, in degrees for horizontal motions, or the characters “UPW” or “DNW” for vertical components.

EXT= 3 characters denoting the file extension, set equal to “MAE”.

For example, IV40ELCN180.MAE is the NS component of ground motion recorded at El Centro in 1940, located in the Imperial Valley of California. The MAE extension denotes the use of the formatting style adopted by USEE.

3.5.1.2 Format of Recorded Ground Motion Files

The suite of recorded ground motions provided with USEE comes from a variety of sources. They have been reformatted according to the convention described in this section. All files begin with a header consisting of any number of lines, each line beginning with the exclamation (“!”) mark. For example, data from the 1940 NS El Centro record is reproduced below:

```
! Mid-America Earthquake Center Format on June 29,1998
! Corrected Recorded Ground Motion
! Units are cm, sec
! GENERAL INFO
! Earthquake: Imperial Valley
! Date: May 19,1940
! Station: El Centro Site Imperial Valley Irrigation District
! Component: N180
! PGA=341.7
! RECORD SOURCE:
! Source: NCEER
! Source Identification:
! EARTHQUAKE DATA:
! Trigger Time:hr|min (24 hr)=0436, sec=41.0  time code=UTC
! Location: latitude=32.8000, longitude=-115.5000, depth (km)=0.0
! Magnitude: ML=6.3  MS=NA  MW=NA
! STATION DATA:
! Station No: 117 , Channel No:
! Location: latitude=32.79528, longitude=-115.54861, elevation (km)=0.0
! RECORD DATA:
! Initial Velocity=-4.664 Initial Displacement=2.159
! Duration of Record (sec)=53.74
! Number of Acceleration points=2688 Time Step (sec)=0.02
! Interpolated
TIME ACCELERATION
```

0.000 -1.400
0.020 -10.800
0.040 -10.100

...
...

The actual file is simple, unformatted ASCII text. The selection above has additional formatting to clarify the information provided. **Bold** text lines identify information that must be supplied for USEE to use the ground motion in response analyses. *Italic* text lines indicate information that if supplied, is extracted from the record for display to the user when the record is selected in the recorded ground motions step. This information is useful but is not required. No restriction is given as to the number and sequence of header lines that begin with an exclamation point (“!”). The line immediately following the last “!” must contain the text “TIME” and “ACCELERATION”. Paired time-acceleration data begin on the second line following the last “!” line and must be in two columns. Units of sec and cm/sec² are assumed. While space must be provided between data columns, no other special formatting of the numerical quantities is necessary.

Selecting the *View Accelerogram* button in the base input step causes a window to appear where the user may view the accelerogram of the selected ground motion. The *View File Header* button may be selected to show the ground motion file information (all lines that begin with a “!”).

Additional motions may be added by the user, and these will be recognized by the program if the ground motion data files are located in the subdirectory with the other recorded ground motions. Each motion must follow the format described above.

3.5.2 Synthetic Motions

Synthetic ground motions were developed by Professor Y.K. Wen and Chiun-Lin Wu in Project Number RR-1 of the Mid-America Earthquake Center and are included in the USEE distributions. The “full” distribution contains the complete catalogue of synthetic motions developed in this project. The motions were developed for rock and soil types at three cities (Memphis, TN, Carbondale, IL and St. Louis, MO) and for different probabilities of exceedence. “Radio” buttons selected by the user identify the desired city, soil type, and exceedence probability. Specification of these parameters determines the synthetic motions listed in the window.

3.5.2.1 Synthetic Motion Filenames

The synthetic motions are stored in the **USEE/waveforms/synthetic** subdirectory. The file names are identical to those used in project RR-1. Each filename contains 7 characters according to the following format: LPR_SQS.MAE where:

L= 1 character representing city location (M for Memphis, C for Carbondale, and L for St. Louis).

P= 2 digits representing the probability of exceedence in a 50-year interval.

SQ= 2 digits representing a sequential number in each earthquake set.

S= 1 character representing the soil type (R for hard rock, S for soil).

MAE= 3 character extension to denote the use of the Mid-America Earthquake Center format

For Example, C02_01S.MAE is a synthetic motion for a soil site in Carbondale having 2% of probability of exceedence in 50 years.

3.5.2.2 Format of Synthetic Motion Files

The synthetic motions conform to a consistent file format. The file header is illustrated below for the C02_01S.MAE file.

```
! Mid-America Earthquake Center Format on December 16, 1999
! Synthetic Motion
! Units are cm, sec
! Source: Mid-America Earthquake Center
! Created by: Prof. Wen, Y.K. in the Project Number RR1 at the MAE Center
! City Location: Carbondale
! Soil Type: Soil
! Exceedence Probability level in 50 yrs: 02% in 50 yrs.
! Focal Depth (km): 17.4
! Epicentral Distance (km): 166.4
! Closest Horizontal Dist to the Surface Projection of Rupture Plane: 106.2
! Deviation from Median Attenuation: 0.90
! Duration: 149.99 sec
! Peak Ground Acceleration: 513.400 cm/sec**2 at time: 9.84 sec
! Peak Ground Velocity: -52.500 cm/sec at time: 10.57 sec
! Peak Ground Displacement: -18.390 cm at time: 16.92 sec
c0611r01 8.0 17.4 166.4 106.2 0.90
  sec    cm/sec**2
  0.00  0.1221E+00
  0.01  0.1231E+00
  0.02  0.1222E+00
  0.03  0.1201E+00
  0.04  0.1198E+00
```

....

....

The header information beginning with the “!” mark was inserted when the motions

were prepared for distribution in USEE. Only the bold text lines are required for USEE to use the synthetic data in the response analyses. No information about the record is displayed to the user in the *Synthetic Motions* tab of the base input window. However, the user may view the file header from this window by clicking the **View File Header** command button. The two lines following the lines beginning with “!” originated in the RR-1 project. The first of these identifies the file ID, moment magnitude, focal depth (km), epicentral distance (km), closest horizontal distance to the surface projection of rupture plane (km), and deviation from median attenuation, ϵ . The second line contains titles for the columns of synthetic motion data. Synthetic motion data begins on the third line. USEE assumes the first column is time, in sec, and the second column is acceleration, in cm/sec^2 .

Selecting the *View Accelerogram* button in the base input step causes a window to appear where the user may view the accelerogram of the selected ground motion. The *View File Header* button may be selected to show the ground motion file information (all lines that begin with a “!”).

3.5.3 Pulses

Several pulse types may be selected for the base input acceleration. These are shown in Figure 10. The motions are specified using several parameters:

- Pulse duration, t_I : duration (in time) of the pulse acceleration.
- Pulse amplitude, a_I : peak value of pulse acceleration.
- Computation time t_{RD} : the duration over which the dynamic response is to be calculated. The computation time must be greater than or equal to the pulse duration. This creates two intervals of motion. Forced vibration occurs for $0 < t < t_I$, and free vibration occurs for $t > t_I$.
- Number of cycles: Partial cycles may be applied by specifying non-integer values. For example, for a half-cycle of a sine wave, 0.5 is specified for the number of cycles.

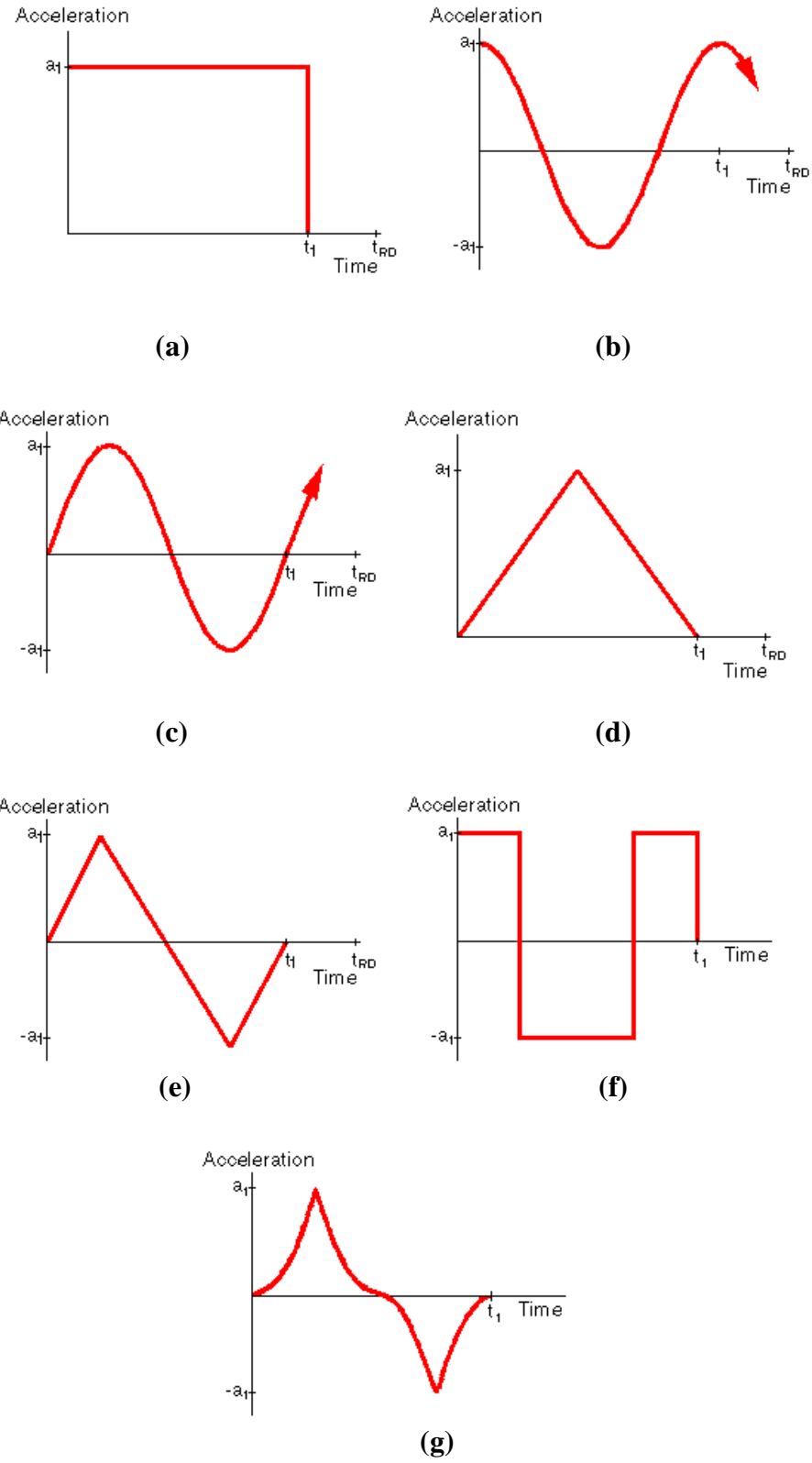


Figure 10. Pulse types

3.5.4 Scale Factors

3.5.4.1 Amplitude Scale Factor

The amplitude scale factor scales the amplitude of the input acceleration. Any non-zero amplitude scale factor may be specified.

3.5.4.2 Time Scale Factor

The time scale factor scales the time coordinates of the acceleration. Values of the time scale factor must be positive.

3.6 Tutorial

Annotated examples are provided in the following to introduce new users to the operation of the USEE. Separate examples are provided to illustrate the *Single-Degree-of-Freedom*, *Approximate Multistory Building*, and *Response Spectra* modules.

To begin, run **USEE** by selecting **Utility Software for Earthquake Engineering** from the **Start** menu. This is a good time to set your preferences of units, parameters, and export options, although they may be changed subsequently without affecting the underlying data. Set the parameters by selecting **Options** from the **Preferences** menu on the menubar. To specify the computation time step, select the **Parameters** tab on the window that appears. Typically, a value not exceeding 10% of the period is used. The program will automatically reduce the time step if required for convergence of the solution. Set the *Computation Time Step* to “0.01” sec. To report results for every computation time step (0.01 sec), select “1” for the *Report Results* box. Enter “1” to set the overshoot tolerance as 1% of the yield displacement. Click on **Export Options** tab to choose what to export from the provided checkboxes. You may set the units you prefer from either the **Units** tab of current window or the **Units** pull-down list box on the toolbar.

3.6.1 SDOF Analysis Example

The first example computes the response of a SDOF system to the 1940 NS El Centro record. The oscillator has an initial period of vibration of 0.75 sec, yield strength equal to 30% of its weight, viscous damping equal to 5% of critical damping, and is modeled as having an elastic-perfectly plastic load-deformation response.

From the main USEE window, select **New Response Analysis** and then select **SDOF Oscillator**. This brings forth a series of windows titled *Step 1* through *Step 3* that are

used for analysis of SDOF systems. Data for this example are entered as follows:

Step 1: This window displays three tabs: *Recorded Ground Motions*, *Synthetic Motions*, and *Pulses*. Since El Centro is a recorded ground motion, select the *Recorded Ground Motion* tab. A list of ground motions is displayed. Select and verify that “IV40ELCN180.MAE” is indeed the record you seek by looking at the information presented on the right side of the screen. Select the *Entire Record* option to analyze response over the entire duration of the record. Set the *Amplitude Scale Factor* and the *Time Scale Factor* to “1.0”. To advance to *Step 2*, click the **Next** button.

Step 2: A linear, bilinear, or stiffness-degrading model must be selected. For elastic-perfectly plastic response, select the bilinear model. Enter “5” to set *Viscous Damping* to 5% of critical damping, enter “0” for the *Post-Yield Stiffness* to obtain elastic, perfectly plastic response, and enter “0.3” for the yield strength coefficient. Either the period of vibration or the yield displacement must be specified. Since the period is 0.75 sec, enter “0.75”. USEE reports the corresponding yield displacement. Click the **Compute Results** command button to advance to *Step 3*.

Step 3: The computed results are displayed in this step. The two plots may be used to display load-deformation response and the displacement or acceleration histories, as well as other quantities. Peak quantities are tabulated. Figure 11 and Figure 12 show load-deformation response and the displacement history for the SDOF example.

After viewing the results, the user may start a new analysis by clicking the **Start New Analysis** button, or may click the **View Summary Log** button to view the input parameters for the current analysis. Response quantities determined during the analysis may be saved to a text file by selecting **Export Output** from the **File** menu. Plots may be copied to the Windows Clipboard using a left mouse click to select the plot and a right mouse click to copy the plot to the Clipboard. The plots may be pasted into other Windows applications from the Clipboard.

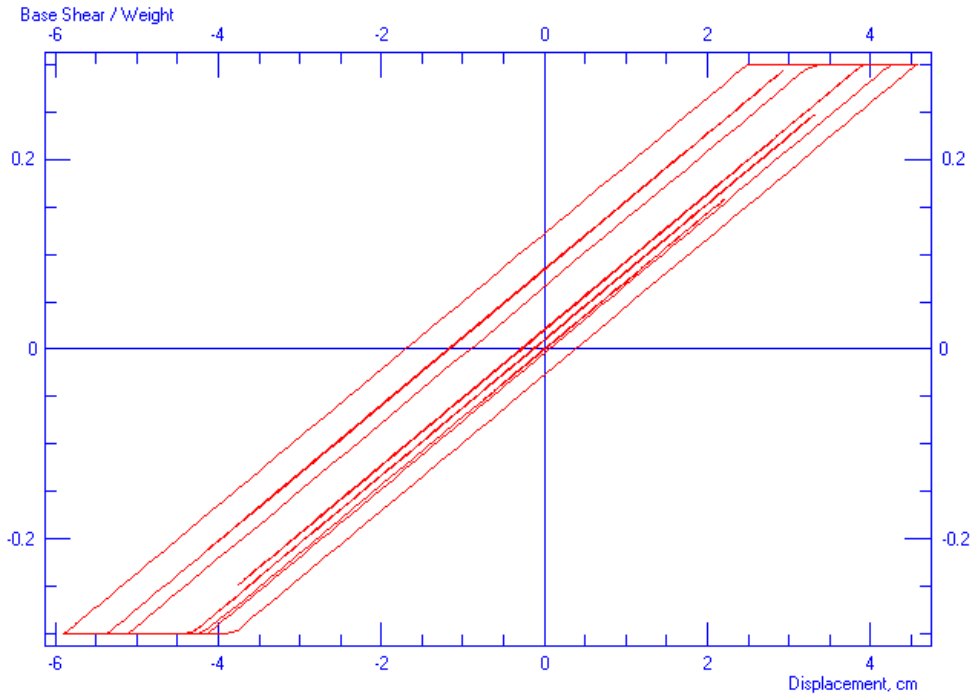


Figure 11. SDOF example: Base Shear / Weight vs. Displacement (cm)

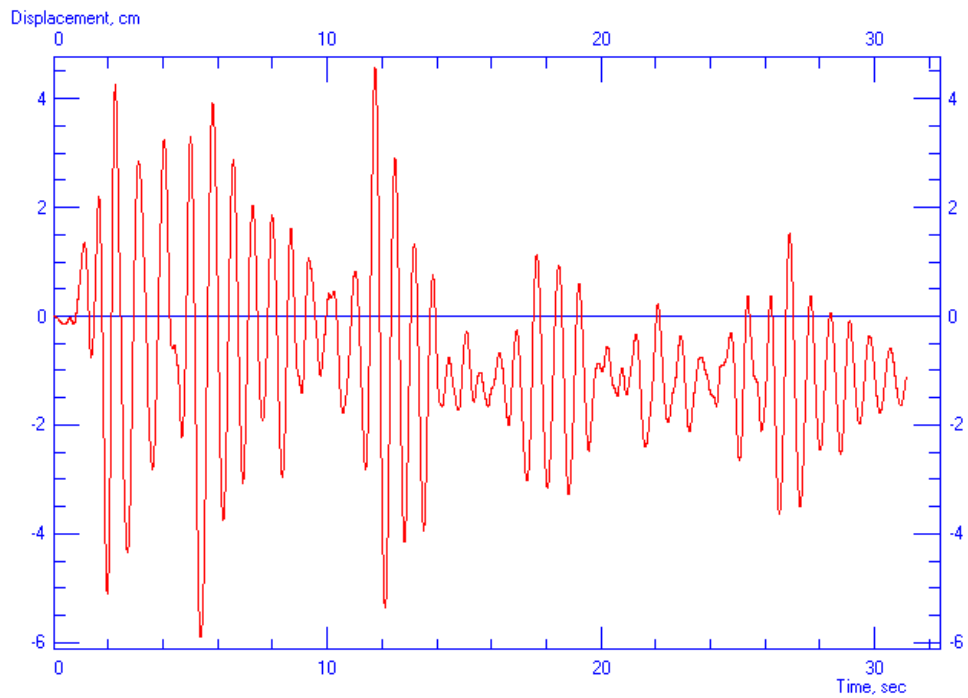


Figure 12. SDOF example: Displacement (cm) vs. Time (sec)

3.6.2 Multistory Building Approximation Analysis Example

The approximate response of a 4-story moment resisting frame structure is computed for the El Centro record. In this example, the drift at yield of the frame is 0.25% of the total building height. The frame has a base shear coefficient at yield equal to 25%, story weights of 318kN, story heights of 4 m, viscous damping equal to 5% of critical damping, and an idealized elastic-perfectly plastic response. The ATC-40 formulation for the base shear strength will be used. Story weights are uniform.

To begin, from the main USEE window, select **New Response Analysis** and then select **Multistory Building Approximation**. This brings forth a series of windows titled *Step 1* through *Step 4* that pertain to the current analysis. Data for this example are entered as follows:

Step 1: This window provides for the input of parameters that describe the building. The number of stories, weight of each story, story heights, and deflected shapes are specified. Since a four-story building will be analyzed, select “4” from the pull down menu labeled *Number of Stories*. Set the story weights equal by selecting the appropriate button in the box labeled *Are Story Weights Equal?* The weight of each story is 318 kN. Next, enter “4” in the text box labeled *Story Height (m)* and make every story this height by selecting the appropriate button. Select the prescribed deflected shape *Shear Beam (Parabolic)* for this analysis, to approximate the response this moment frame. Click the *Next* command button to advance to *Step 2*.

Step 2: This window displays three tabs for specifying the base input acceleration: *Recorded Ground Motions*, *Synthetic Motions*, and *Pulses*. Since in this example the base input is a recorded ground motion, select the *Recorded Ground Motion* tab. A list of the recorded ground motions is presented. Select IV40ELCN180.MAE (1940 NS El Centro record) from list. Select the *Entire Record* option to compute response for the entire record duration. Enter “1.0” for the *Amplitude Scale Factor* and the *Time Scale Factor*. Click the **Next** button.

Step 3: The user must select one of the linear elastic, bilinear, and stiffness-degrading load-deformation models. For this example, select the bilinear model. Enter “5” for *Viscous Damping* and “0” for *Post-Yield Stiffness*. In this example, C_y^* will be computed as per ATC-40, so select the corresponding radio button. The user must specify the drift at yielding, so enter 0.25 in the corresponding text box and enter “0.25” for C_y . Click the **Compute Results** command button to advance to *Step 4*.

Step 4: The results are displayed in *Step 4*. Figure 13 and Figure 14 show load-deformation and displacement response history of the building. The base shear coefficient and roof displacement are point of interest.

After viewing the results, the user may start a new analysis by clicking the **Start New**

Analysis button. Clicking the **View Summary Log** button allows the user to view the input parameters for the current analysis. Response quantities of the building may be saved to a text file by selecting **Export Output** from the **File** menu.

3.6.3 Response Spectra Examples

The computations of three types of response spectra are illustrated for the 1940 NS El Centro in this example. The first example considers linear behavior for three viscous damping values equal to 0%, 2%, and 10% of critical damping. In the second example, elastic-perfectly plastic behavior is considered, with yield strengths equal to 25%, 50%, and 100% of the oscillator weight. Viscous damping is assumed to be 5% of critical damping. In the third example, elastic-perfectly plastic behavior is considered and ductility is held constant, equal to 2, 4, and 8. Viscous damping of 5% of critical damping is assumed. The spectra are computed for 60 uniformly spaced periods ranging from 0.05 to 3 seconds.

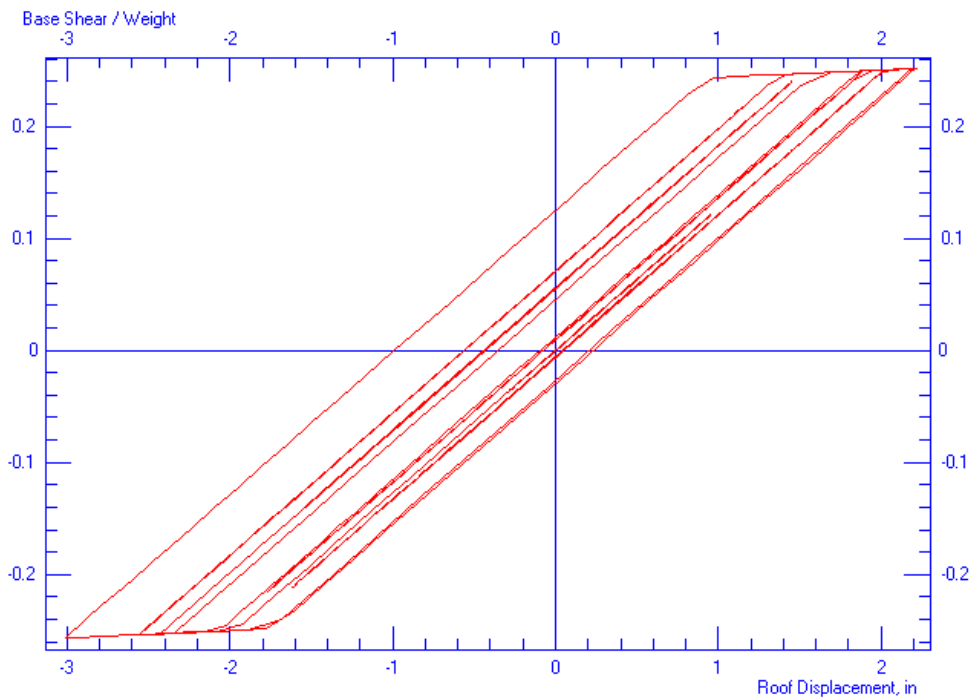


Figure 13. Multistory building approximation example: Base Shear / Weight vs. Roof Displacement, (cm)

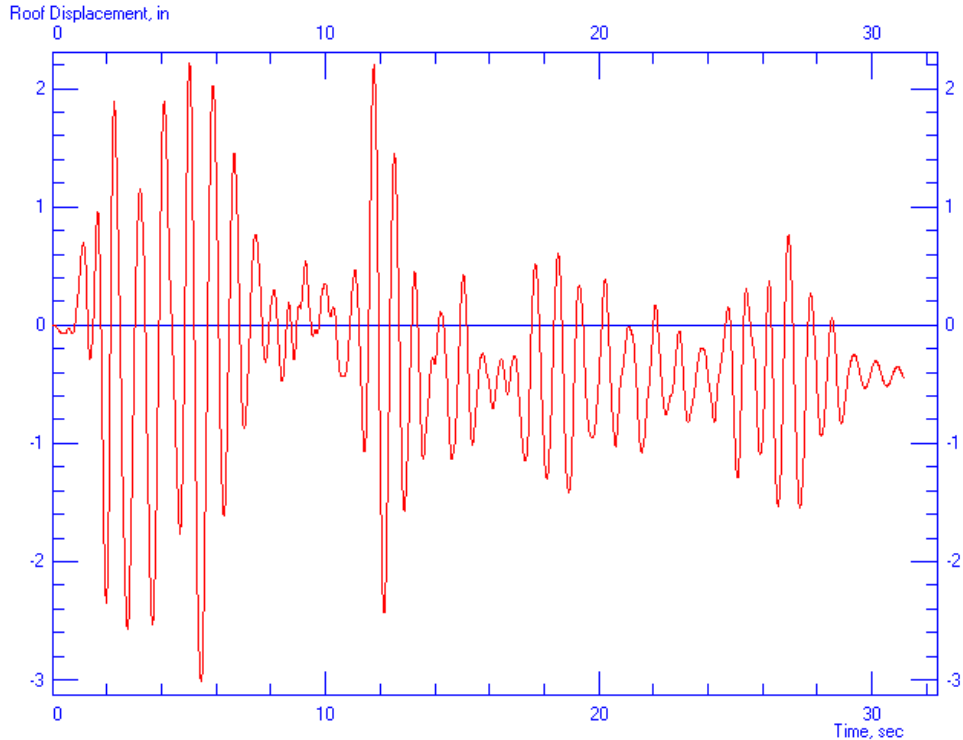


Figure 14. Multistory building approximation example: Roof Displacement (cm) vs. Time (sec)

To begin, from the main USEE window select **New Response Analysis** and then select **Response Spectra**. This brings forth a series of windows titled *Step 1* through *Step 3* that pertain to the current analysis. Data for the first example are entered as follows:

Step 1: This window displays three tabs: *Recorded Ground Motions*, *Synthetic Motions* and *Pulses*. Since in this example, the base input is a recorded ground motion, select the *Recorded Ground Motion* tab. A list of recorded ground motions is presented. Select “IV40ELCN180.MAE” record from the list. Select the **Entire record** button to compute response for entire record duration. Enter “1.0” for both the *Amplitude Scale Factor* and the *Time Scale Factor*. Click the **Next** button to advance to *Step 2*.

Step 2: Among the linear, bilinear, and stiffness-degrading models, select the linear model. Next, specify the periods by selecting the **uniformly spaced** radio button and entering “60” periods ranging from “0.05” to “3” seconds. For the parameter to vary, *Viscous Damping* is the only choice when linear behavior is assumed. Choose “3” discrete values from the pull down menu and enter the values of “0”, “2”, and “10” in the text boxes labeled *Values*. Click the **Compute Results** command button.

Step 3: The results of the response spectrum computations are displayed in *Step 3*. Spectra corresponding to each parameter value are displayed with the color indicated at the top of the window. Select the **Zoom to Full Screen** button to enlarge the plot. Lines are plotted for each parameter value with a different color. Figure 15 shows spectral acceleration versus period for damping values of 0%, 5%, and 10%.

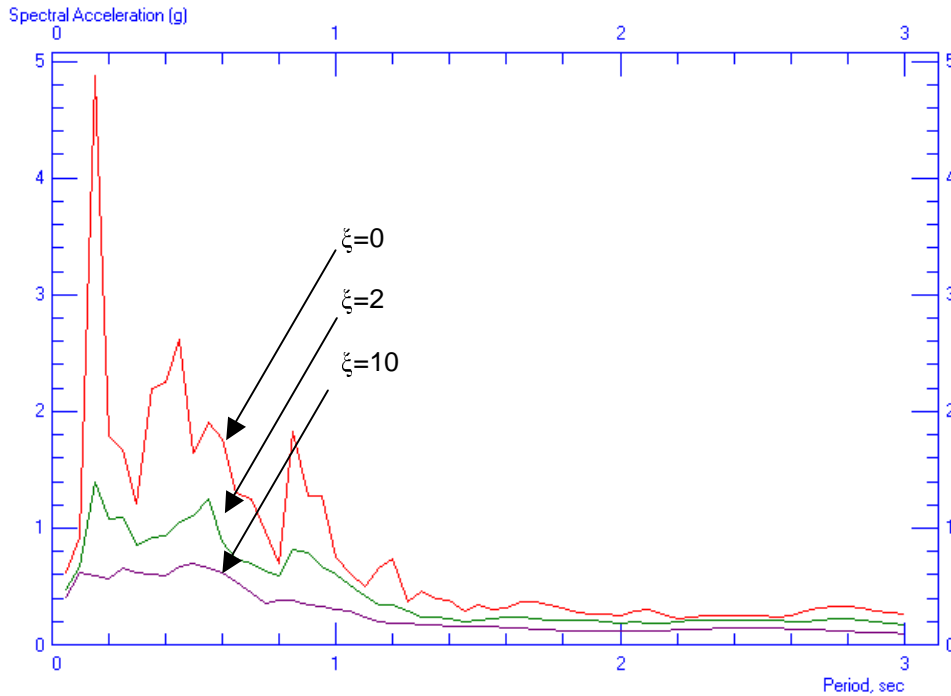


Figure 15. Response spectra example: Spectral Acceleration (g) vs. Period (sec)

This completes the first example. To modify the current analysis to begin the second analysis, click on the **Back** button on the *View Results* window. This takes the user back to *Step 2*.

Step 2: Among the linear, bilinear, and stiffness-degrading models, select the bilinear model. Next, specify the periods by selecting the **uniformly spaced** radio button and enter “60” periods ranging from “0.05” to “3” seconds. For the parameter to vary, select the *Yield Strength Coefficient*. Choose “3” discrete values from the pull down menu and enter the values of “0.25”, “0.50”, and “1.00” in the text boxes labeled *Values*. For *Viscous Damping* enter “5”, and enter “0” for *Post-Yield Stiffness*. Click the **Compute Results** command button.

Step 3: The results of the response spectrum computations are displayed in *Step 3*. Spectra corresponding to each parameter value are displayed with the color indicated at the top of the window. Select the **Zoom to Full Screen** button to enlarge the plot. Lines are plotted for each parameter value with a different color. Figure 16 shows ductility versus period for the yield strength coefficient values of 0.25, 0.50, and 1.00.

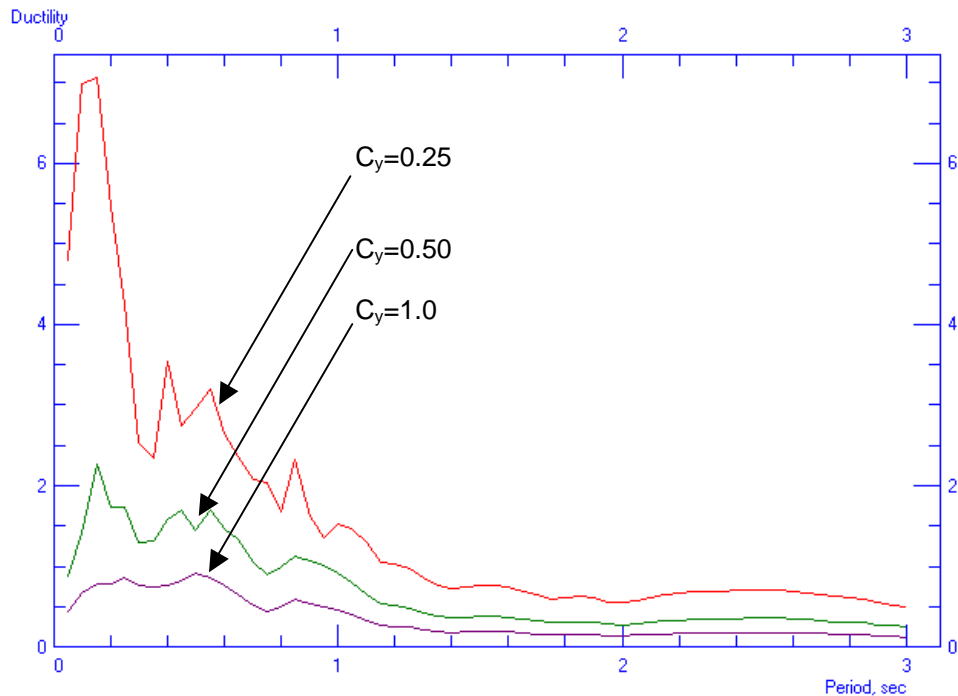


Figure 16. Response spectra example: Ductility vs. Period (sec)

This completes the second example. To modify the current analysis to begin the third example, click on the **Back** button on the *View Results* window. This takes the user back to *Step 2*.

Step 2: Among the linear, bilinear, and stiffness-degrading models, select the bilinear model. Next, specify the periods by selecting the **uniformly spaced** radio button and entering “60” periods ranging from “0.05” to “3” seconds. For the parameter to vary, select *Constant Ductility Factor*. Choose “3” discrete values from the pull down menu and enter the values of “2”, “4”, and “8” in the text boxes labeled *Values*. For *Viscous Damping* enter “5”, and enter “0” for *Post-Yield Stiffness*. Click the **Compute Results** command button.

Step 3: The results of the response spectrum computations are displayed in *Step 3*. Spectra corresponding to each parameter value are displayed with the color indicated at the top of the window. Select the **Zoom to Full Screen** button to enlarge the plot. Lines are plotted for each parameter value with a different color. Figure 17 plots yield strength coefficient versus period for the ductility values of 2, 4, and 8. The yield strength coefficient is also plotted against yield displacement in Figure 17.

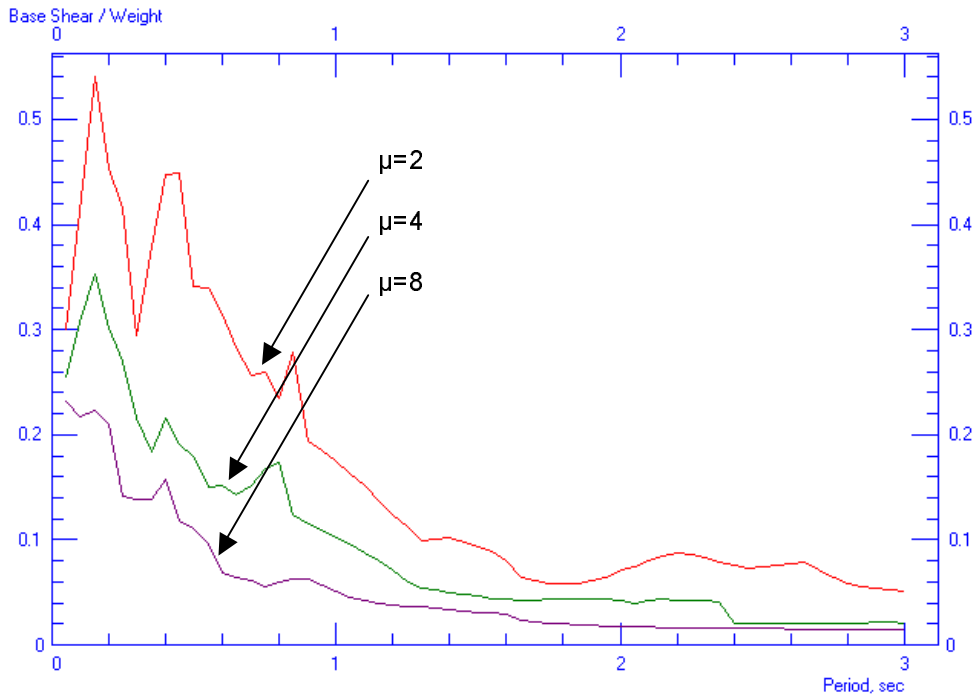


Figure17. Traditional Constant Ductility Spectra: Base Shear / Weight vs. Period (sec)

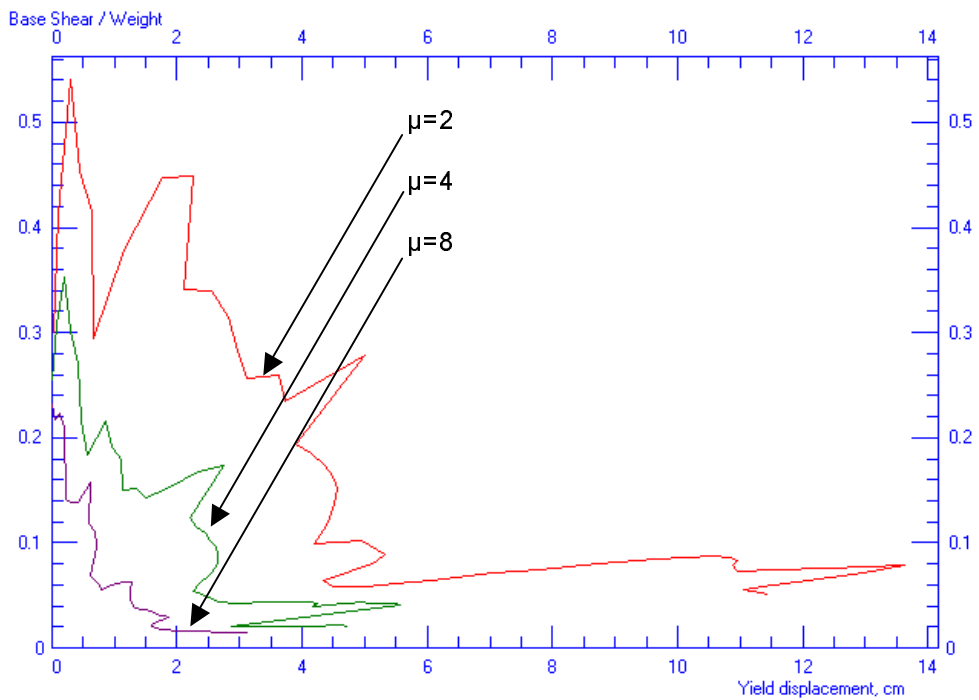


Figure18. Yield Point Spectra: Base Shear / Weight vs. Yield Displacement (cm)

4 Program Verification

4.1 Accuracy of Computational Engine

To validate the accuracy of the USEE computations, response was computed for selected cases that are reported in *Dynamics of Structures* (Chopra, 1995). Response for these cases also was computed using NONSPEC (Mahin and Lin, 1983) and NONLIN (Charney et al, 1998). Table 3 shows the properties of SDOF systems considered. The SDOF systems with bilinear load-deformation response were modeled as elastic-perfectly plastic. All cases are subjected to the 1940 NS El Centro record that is described in *Dynamics of Structures* (Chopra, 1995). The results are summarized in the table below.

Table 3. Validation of SDOF code

		SDOF Properties			Peak Displacement, cm			
		T (sec)	ξ %	Fy / W	USEE	Chopra book	NONSPEC	NONLIN
Linear	1	0.5	2	----	6.83	6.78	6.83	7.11
	2	1.0	2	----	15.16	15.16	15.16	15.57
	3	2.0	2	----	18.98	18.97	18.97	19.63
	4	2.0	0	----	25.19	25.17	25.19	26.29
Bilinear	1	0.5	0	0.170	4.37	4.34	4.37	4.50
	2	0.5	5	0.125	4.70	5.26	4.70	5.00
	3	0.5	5	0.250	4.55	4.45	4.55	4.45
	4	0.5	5	0.500	4.50	4.11	4.50	4.37
	5	0.5	5	1.000	5.72	5.72	5.72	5.82

The computation engine of USEE is a C++ version of the original Fortran code used in NONSPEC. The peak displacement results of USEE and NONSPEC in Table 3 are different only in the 4th digit of precision, presumably due to roundoff error or other minor differences. For linear elastic cases the USEE and Chopra text report similar results; these results differ somewhat from those computed with NONLIN. For inelastic response, the results do not show the same level of agreement. There are several reasons that might cause these differences. Although, the same computational time step values are used for computed results of USEE, NONSPEC, and NONLIN, time step values used for the results reported by Chopra were not identified. Also, USEE and NONSPEC reduce the time step values in regions where smaller time steps are required for convergence. It is not clear whether NONLIN and the code used by Chopra reduce the time steps in these regions, since published information does not address this issue. Figures 19 and 20

compare the displacement history and base shear versus displacement response for the bilinear case having a period of 0.5 sec, yield strength coefficient of 0.170, and damping value of zero percent.

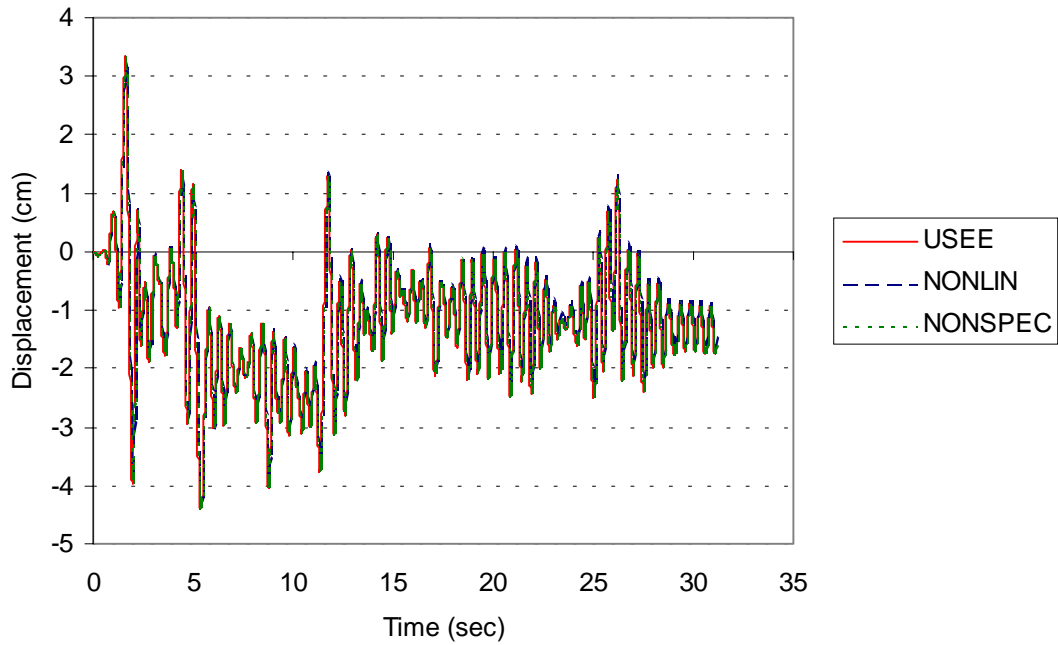


Figure 19. Comparison of USEE to NONLIN and NONSPEC: Displacement (cm) vs. Time (sec)

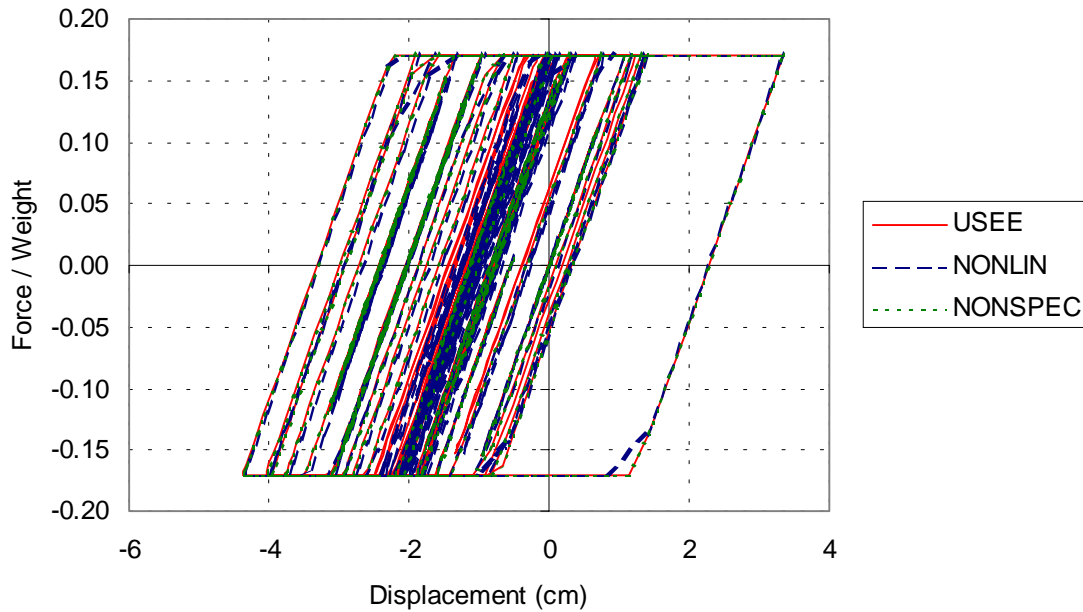


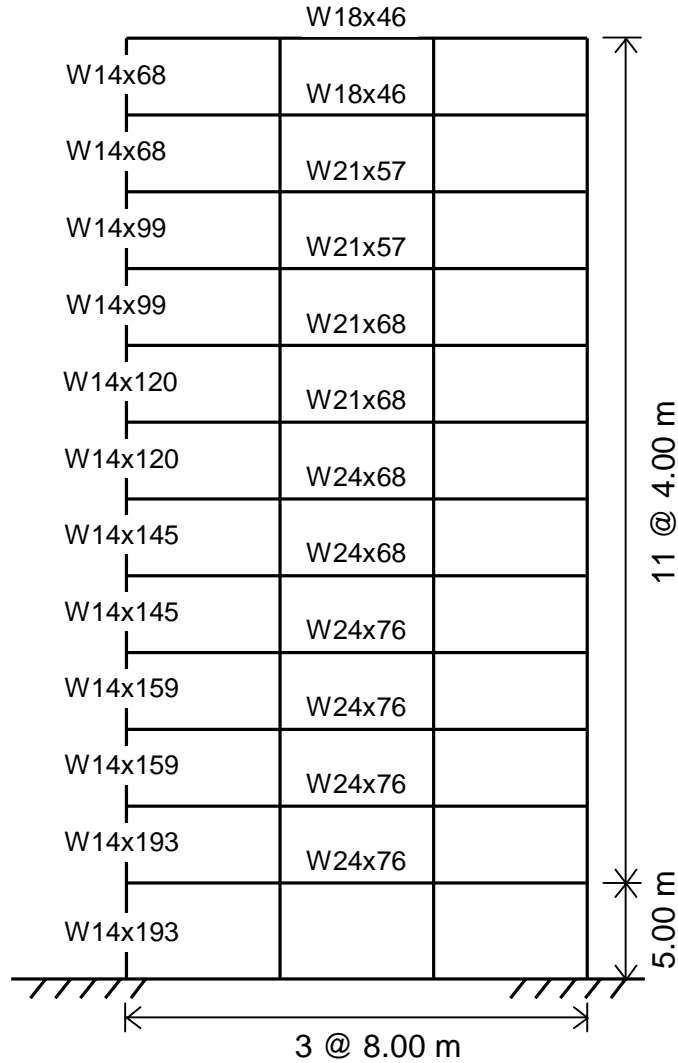
Figure 20. Comparison of USEE to NONLIN and NONSPEC: Force / Weight vs. Displacement (cm)

4.2 Accuracy of Multistory Building Approximation Analysis: Example

“Equivalent” SDOF models of multistory buildings are useful for estimating the peak displacements and displacement response histories (e.g. Saiidi and Sozen (1981), Fajfar and Fischinger (1988), Qi and Moehle (1991), Miranda (1991), and Lawson et al. (1994)). The use of such “equivalent” systems has been formalized in ATC-40 (1996) and FEMA-273/274 (1997). In this section, the response of a 12-story moment-resistant frame building computed using Drain-2DX (Prakash, et al, 1993) is compared to the response computed using a SDOF analogue in the *Multistory Building Approximation* analysis module. The El Centro ground motion was applied to the building frame with amplitude scaled by a factor of 2.

The 12-story steel moment-resistant frame building (Figure 21) was designed for uniform floor masses equal to 551 kN per floor. The base shear strength was established to limit drift response; the design is described in more detail as the “Flexible-12” frame in

Black and Aschheim (2000). The frame was designed only for lateral loads in order to validate a design methodology. Lateral response was computed using DRAIN-2DX (Prakash, et al, 1993). Flexural response was modeled using beam-column elements



Note: all columns and all beams within a story are identical.

Figure 21. Multistory building approximation analysis example

(Type 02) extending along beam and column centerlines; the post-yield stiffness was set equal to 5% of the initial stiffness. The first mode of vibration has a period of 2.168 sec and the first mode shape is shown in Figure 22.

In the present case, the first elastic mode shape was considered an adequate approximation of the predominant mode shape. This results in the same period of vibration for the multi-degree-of-freedom system and its “equivalent” system when the ATC-40 procedure is used. The load-deformation response of the building frame was obtained using a nonlinear static (pushover) analysis that was done by applying lateral forces in proportion to the mode shape amplitude and mass at each floor level (Figure 23) using DRAIN-2DX. A bilinear curve was fit to the capacity curve to determine the yield strength and displacement for response in the first mode. The displacement of the roof at yield is 0.353 m, or 0.72% of the height of the building, and the base shear coefficient at yield is 0.173. The post-yield stiffness is 17.5% of the initial stiffness.

The response of the building frame was estimated using the *Multistory Building Approximation* analysis module of USEE. In step 1 of the USEE module, a user-defined mode shape was selected and values from Table 4 are used to specify the elastic first mode shape. In the second step, the El Centro record was selected, scaled by a factor of 2. Load-deformation properties established from Figure 22 were specified in the third step. A bilinear model was selected, specifying a base shear coefficient at yield of 0.173, a post-yield stiffness of 17.5% of the initial stiffness, and damping equal to 5% of the critical damping. Either period or yield drift of the frame can be specified for the ATC-40 implementation. Since the elastic first mode shape was used, the period associated with the first mode shape was specified as 2.17 sec. The response computed using USEE is compared with the response computed in the nonlinear response of the MDOF system (using DRAIN-2DX) in Figures 24 and 25. Figure 24 compares the roof displacement histories. Figure 25 compares the base shear versus roof displacement, respectively. From the figures, it can be observed that the roof displacement history of the “equivalent” SDOF model captures the essence of the roof displacement response determined for the MDOF system. However, base shear versus roof displacement response is poorly represented by the “equivalent” SDOF system. While the base shear – roof displacement histories are dissimilar, it may be observed that the estimate based on the “equivalent”

SDOF system provides reasonable estimates of the peak quantities. Although, the “equivalent” SDOF bounds the response, the details of the load-deformation response of the “equivalent” SDOF model and MDOF model are very different.

The goodness of the displacement history shown for the 12-story steel moment-resistant frame building demonstrates that the “equivalent” SDOF model based on the first mode shape can be useful for estimating peak roof displacement and roof displacement histories.

Table 4. First elastic mode shape of the 12-story building frame

Story Level	Normalized 1 st Mode Amplitude
12	1.0000
11	0.9546
10	0.8868
9	0.8120
8	0.7254
7	0.6356
6	0.5409
5	0.4492
4	0.3556
3	0.2640
2	0.1704
1	0.0828

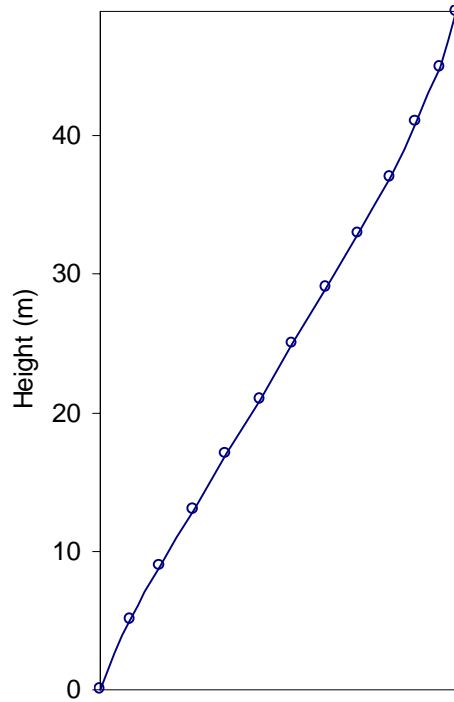


Figure 22. First elastic mode shape of the 12-story building frame

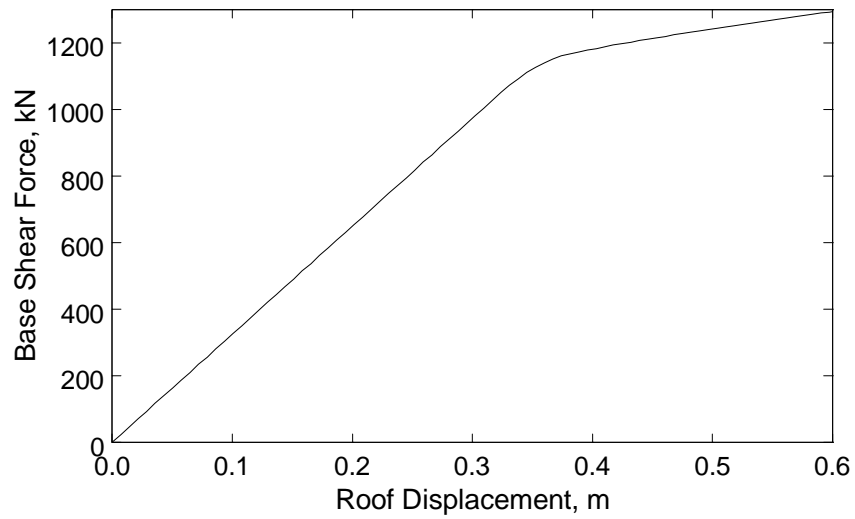


Figure 23. Capacity curve obtained by applying forces proportional to the product of the elastic modal amplitude and mass at each floor in a nonlinear static (pushover) analysis

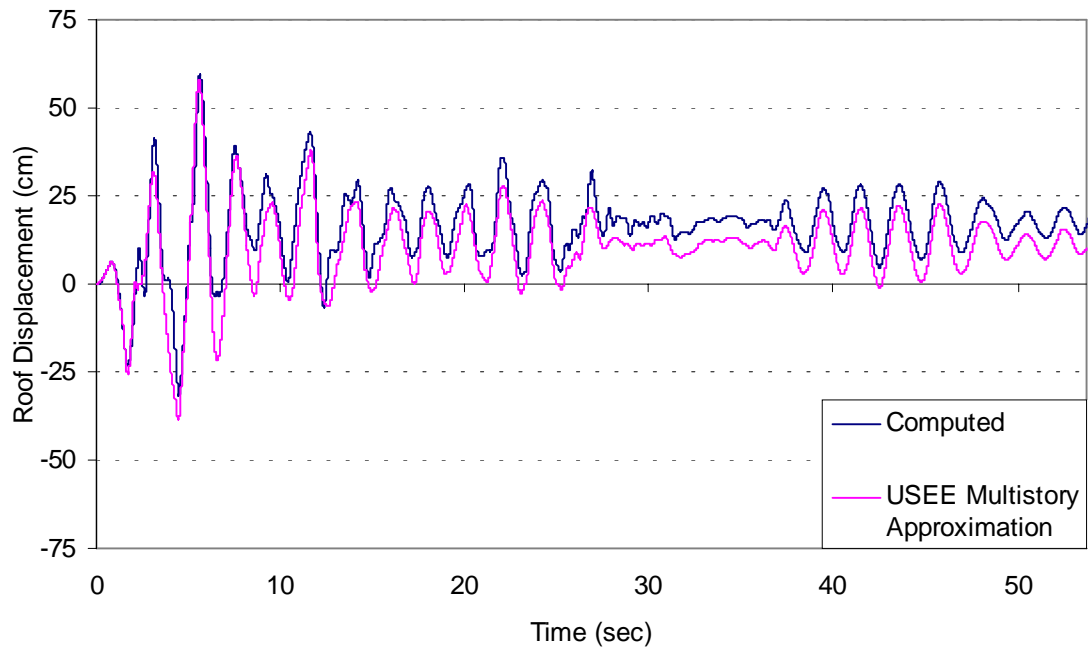


Figure 24. Displacement history of a 12-story building frame subjected to 1940 El Centro record (amplitude scaled by factor of 2)

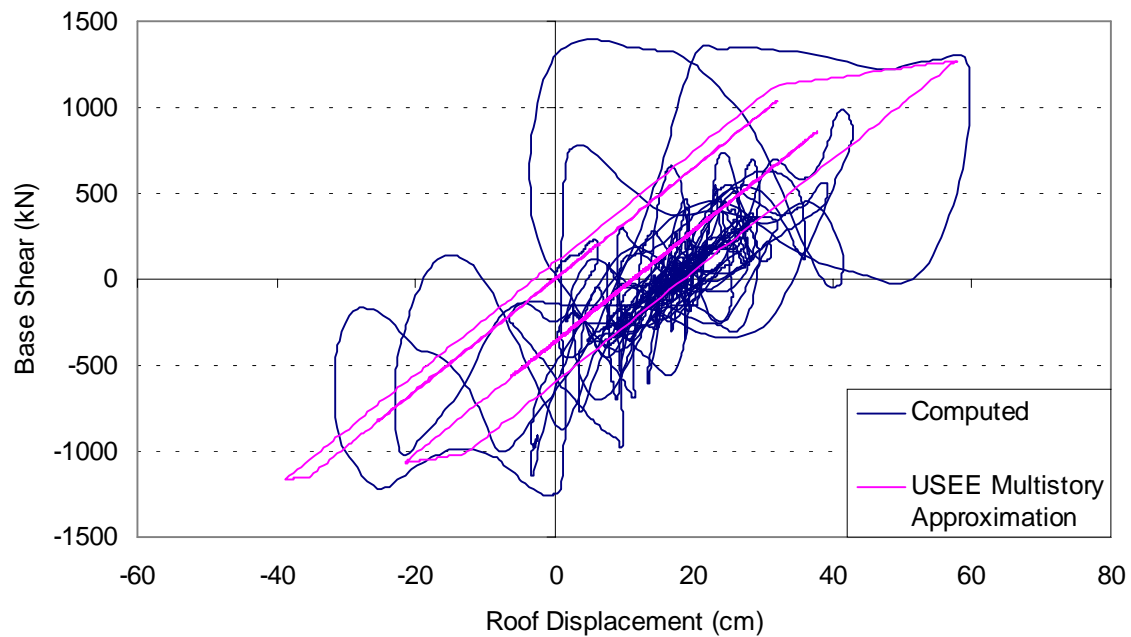


Figure 25. Base shear vs. roof displacement response of the 12-story building frame subjected to 1940 El Centro record (amplitude scaled by factor of 2)

APPENDIX A: Software Development Tools

The computational engine of USEE was written in C++. The code follows the algorithms used by Mahin and Lin (1983). Algorithms introduced for constant ductility iterations are described in Appendix B. The graphic interface for USEE was created using Microsoft Visual Basic 6.0. Dynamic Link Libraries (DLL) are used to communicate between the interface and engine. USEE *Help* was developed using VB HelpWriter Software. The following versions of these programs were used for development of USEE 2001.

Microsoft Developer Studio 97 for DLL files

Microsoft Visual Basic 6.0 (SP3) with Service Pack 3 for graphical user interface

VB HelpWriter Version 4.2.11 for USEE *Help*

USEE utilizes two Dynamic Link Library (DLL) files. One is for computation and the other is for manual testing of the load-deformation models. The code for the load-deformation models is identical in both DLLs.

APPENDIX B: Algorithm for Computing Isoductile Response Spectra

B.1 Introduction

Methods for computing the linear elastic response of a single-degree-of-freedom (SDOF) oscillator to a given ground motion were established in the late 1950s (e.g. Newmark, 1959) and were subsequently extended to oscillators having nonlinear load-deformation relationships (e.g. Veletsos and Newmark (1964), Wilson et al. (1973), and Petkov and Ganchev (1998)). In these methods, the response is computed in the time domain by a series of sequential analyses, each covering a small increment of time Δt .

Of particular interest is the relationship between the strength of the oscillator and the degree of nonlinear behavior that develops. As noted by Newmark and Riddell (1979), the same ductility demand may result for different oscillator strengths. Since the usual design objective is to ensure that ductility demands greater than the target ductility do not develop, selecting the largest of the strengths that result in the target ductility demand is a useful strategy to ensure that the actual ductility responses do not exceed the target ductility, considering that the actual structural properties or ground motions may differ, even slightly, from those assumed in the analysis. An efficient algorithm is necessary, because results are often sought for a large number of periods, for different target ductility values, and for different ground motions, potentially requiring many thousands of nonlinear SDOF analyses.

Although algorithms for determining constant ductility strengths have been developed for research (e.g. Newmark and Hall (1973) and Vidic et al. (1994)) into R - μ - T relations (strength reduction factor as a function of ductility and period), for example, and have been implemented in various software programs (e.g. PCNSPEC (Borosheck and Mahin, 1991) and BISPEC (Hachem, 2000)), few, if any, have received formal attention in the literature. The present algorithm is implemented in USEE for computation of isoductile (constant ductility) response spectra.

B.2 Properties of the Strength-Ductility Relationship

The dynamic response of a SDOF oscillator to a specified excitation is a function of its mass, damping, and load-deformation relation. The load-deformation relation often is idealized as a continuous assembly of piecewise linear segments. Figure B1 (a) shows the yield strength of the oscillator (F_y) and yield displacement (Δ_y), as well as a peak

displacement (Δ_u). The post-yield stiffness (αK) is expressed as a fraction α of the initial stiffness K , and the initial (elastic) period of vibration T is given by $T= 2\pi(M/K)^{0.5}$, where $M=$ the mass of the SDOF oscillator.

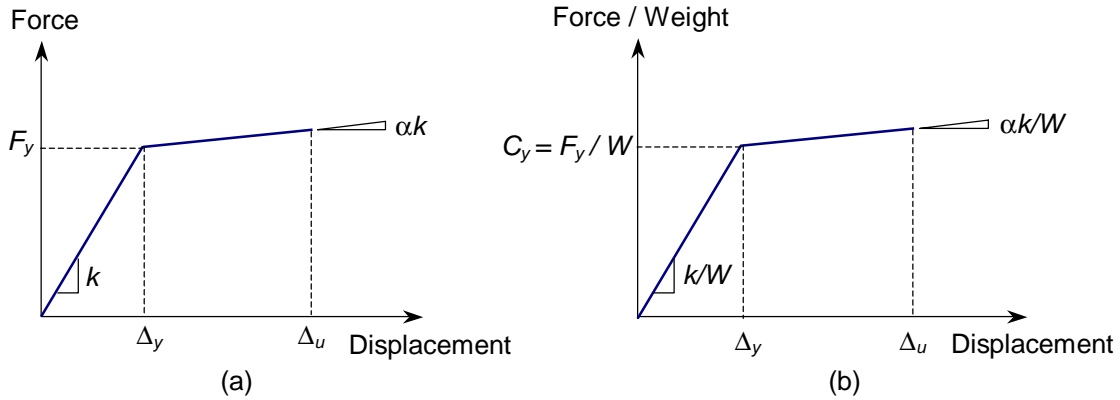


Figure B1. (a) Schematic load-deformation response, and (b) normalized load-deformation response.

A normalized form of the load-deformation relationship may be obtained by dividing the lateral force by the weight of the mass. Doing so allows the load-deformation relation to be expressed in Figure B1 (b) in terms of the yield strength coefficient, C_y , where

$$C_y = \frac{F_y}{W} \quad (\text{B1})$$

and $W= Mg$, where $g=$ the acceleration of gravity. The dynamic response to a base excitation (Figure B2) may be considerably more complex, but even so, the above terms define the oscillator characteristics and intensity of peak response. The displacement ductility, μ , that develops at the peak displacement is given by

$$\mu = \frac{\Delta_u}{\Delta_y} \quad (\text{B2})$$

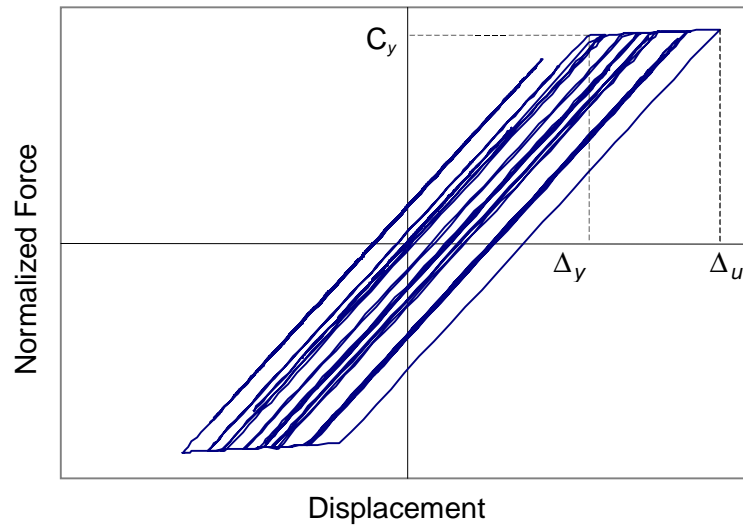


Figure B2. Computed load-deformation response to 1992 Landers earthquake at Joshua Tree Fire Station (NS), for a 1-second period oscillator

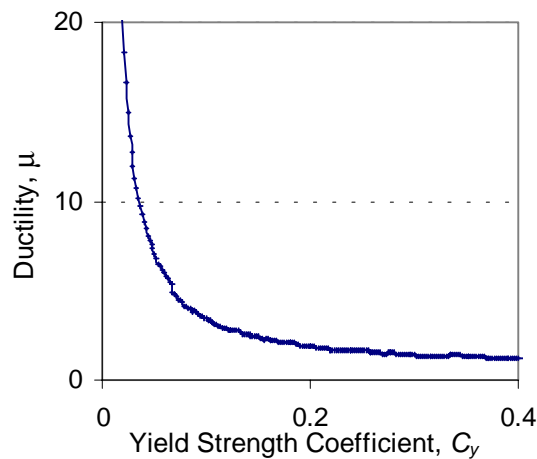


Figure B3. The strength-ductility relationship for a bilinear oscillator having a period of $T= 0.15$ sec responding to the 1987 Whittier Narrows record

The inverse problem, with which this Appendix is concerned, is to determine the strength coefficient, C_y , which causes μ to be equal to a specified value. Figure B3 illustrates the well-known trend that μ increases as C_y decreases. Upon first inspection, a reasonable solution strategy might be to compute the ductilities obtained for arbitrarily chosen strengths, interpolating until a solution of adequate precision is obtained. However, several properties of the strength-ductility relationship require that a more

sophisticated solution strategy be employed:

- Multiple solutions may exist. Figure B4(a) shows the strength-ductility relationship for a bilinear oscillator having $T= 0.20$ sec responding to the NE component of the 1987 Whittier Narrows earthquake recorded at the Mt. Wilson – Caltech Seismic Station. In this case, a peak ductility of 1.4 is obtained for several different strengths; the largest yield strength coefficient is more than 40% greater than the smallest yield strength coefficient. Reporting any one of these strength coefficients as the answer would introduce a degree of arbitrariness to the solution, and would lead to inconsistencies in the results computed using different codes.

As a matter of engineering practice, to ensure that ductilities no larger than the specified value develop, the largest strength corresponding to the target ductility should be identified by the algorithm, indicated by Point A in the figure. An efficient algorithm must strike a balance between the computational cost of obtaining better resolution of the strength-ductility relationship and the possibility of not identifying a higher strength solution.

- An exact solution may not exist. Figure B4(b) shows a close-up view of the strength-ductility relationship in the vicinity of $\mu= 2$ for an oscillator having $T= 0.15$ seconds responding to the same record of the 1987 Whittier Narrows earthquake. Several discontinuities in the ductility response are apparent upon close inspection. If the target ductility lies on a discontinuity, then an exact solution may not be available. For example, Figure 5b indicates that no oscillators exist that respond to this earthquake record with a peak ductility response of exactly 2, for the damping and load-deformation model considered.

Given this finding, instead of requiring an exact solution, the algorithm should identify the strength coefficient for which the ductility is nearly equal to, but does not exceed, the specified target value. Such an algorithm would identify Point A in Figure B4(b) as the solution.

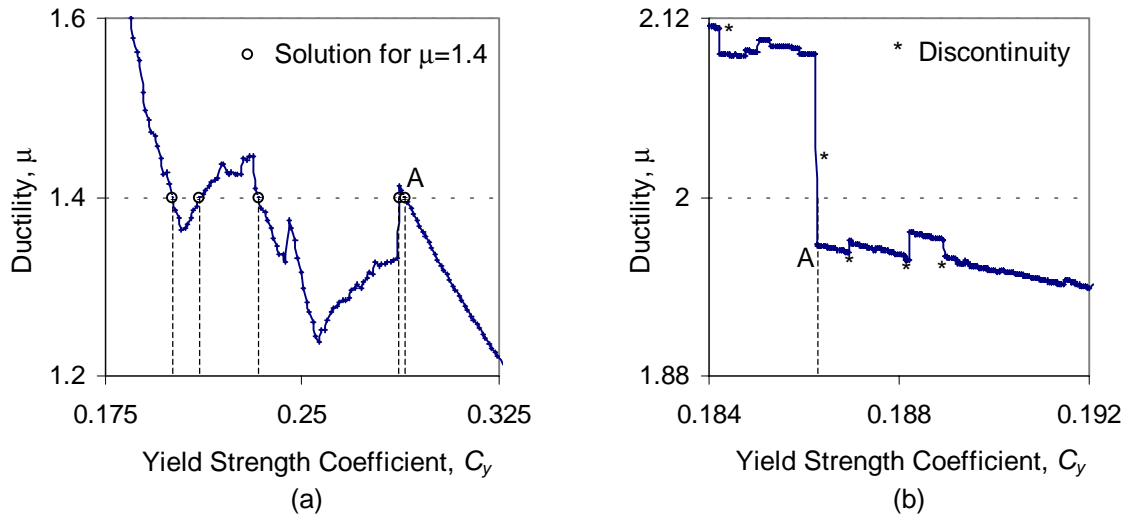


Figure B4. The strength-ductility relationship for a bilinear oscillator responding to the 1987 Whittier Narrows record for an oscillator period of: (a) 0.20 sec, and (b) 0.15 sec.

B.3 Description of the Algorithm

An efficient algorithm is desirable, because many nonlinear response computations may be required to compute constant ductility response spectra. Figure B5 shows the strength-ductility relation in the vicinity of a target ductility, μ_t , for a particular oscillator and ground motion. Nonlinear SDOF analyses at $C_{y,u}$ and $C_{y,l}$ determined the corresponding ductility responses indicated by dark circles in the figure. Simple interpolation between these points would lead to the solution identified by “C” in the figure, missing the higher strength solutions at “A” and “B.” Greater resolution of the strength-ductility relation would provide greater certainty that an unrecognized higher strength solution would not be missed, but this certainty comes at the cost of a larger number of nonlinear SDOF response computations. Thus, a balance must be struck between the time required to obtain a solution and the possibility that an unrecognized higher strength solution may exist. To address this, a two-phase solution procedure is employed. The first phase identifies the region in which a solution is to be obtained. This is done by applying a “check-reject” test to determine if a higher-strength region might contain a solution. If the test determines that an unrecognized higher strength solution is unlikely, the higher strength region is rejected. This process is applied to narrow the bounds on the solution. Once the initial bounds are narrowed sufficiently, the second

phase is begun. In the second phase, a bisection approach is applied to determine a solution as rapidly as possible, within the bounds determined by the first phase. The two phases of the algorithm are described next.

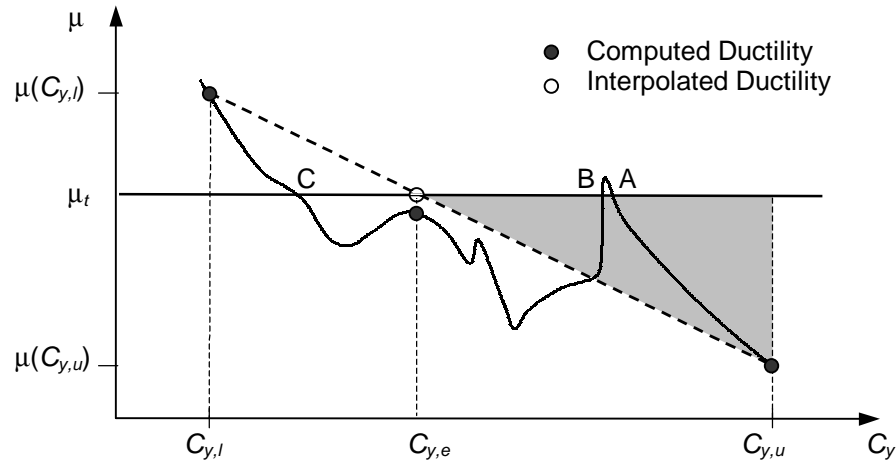


Figure B5. Linear interpolation between $C_{y,u}$ and $C_{y,l}$

B.3.1 Initial Bounding of Solution

The first phase of the algorithm narrows the interval in which the solution lies; the objective is to discard regions of C_y in which it is determined that a solution is unlikely to be found. The algorithm is described in detail in Figure B6. Key concepts are described below.

To begin, the upper bound of the interval, $C_{y,u}$, is set equal to the strength coefficient required for elastic response. This value is determined by computing the response of a linear elastic oscillator having the same period of vibration and viscous damping. The lower bound of the interval, $C_{y,l}$, must result in a ductility greater than the target ductility, to ensure that a solution lies between $C_{y,l}$ and $C_{y,u}$. Experience indicates that $C_{y,l}$ should

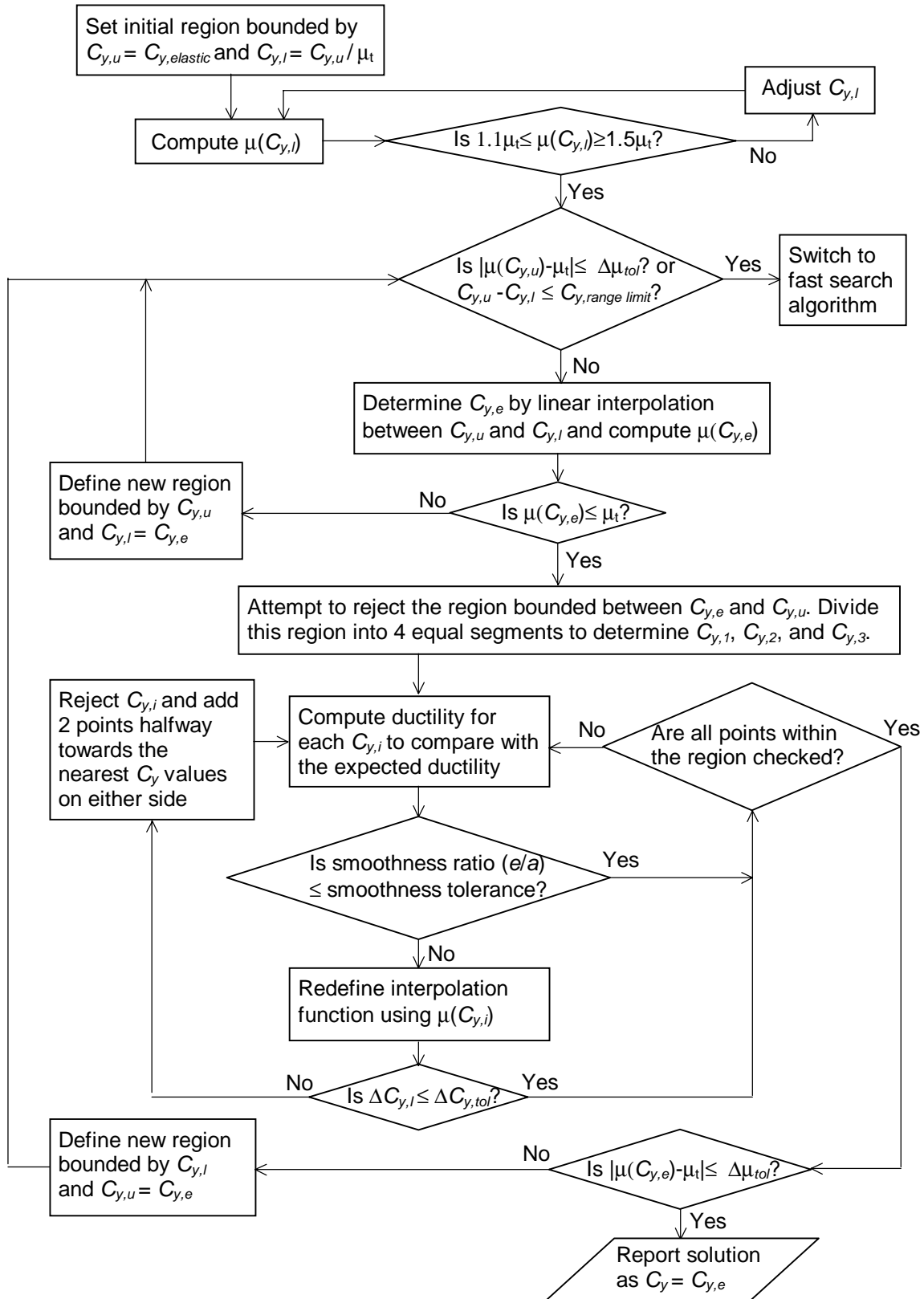


Figure B6. The first phase of the algorithm, for determining the initial bounds on the solution

be selected to result in a ductility $\mu(C_{y,l})$ equal to 1.1 to 1.5 times the target ductility, μ_t . To secure this result, $C_{y,l}$ is estimated initially as $C_{y,u}/\mu_t$ and then is adjusted until $1.1(\mu_t) < \mu(C_{y,l}) < 1.5(\mu_t)$.

Next, linear interpolation between the current upper and lower bound strength coefficients is used to determine an expected solution $C_{y,e}$. The ductility corresponding to $C_{y,e}$ is computed. The computed ductility, $\mu(C_{y,e})$ is compared to the target ductility. The case $\mu(C_{y,e}) > \mu_t$ is illustrated in Figure B7. In this case, the highest strength solution clearly lies between $C_{y,e}$ and $C_{y,u}$. Therefore, the solution bounds are revised by setting $C_{y,l} = C_{y,e}$, and the algorithm restarts with the new bounds.

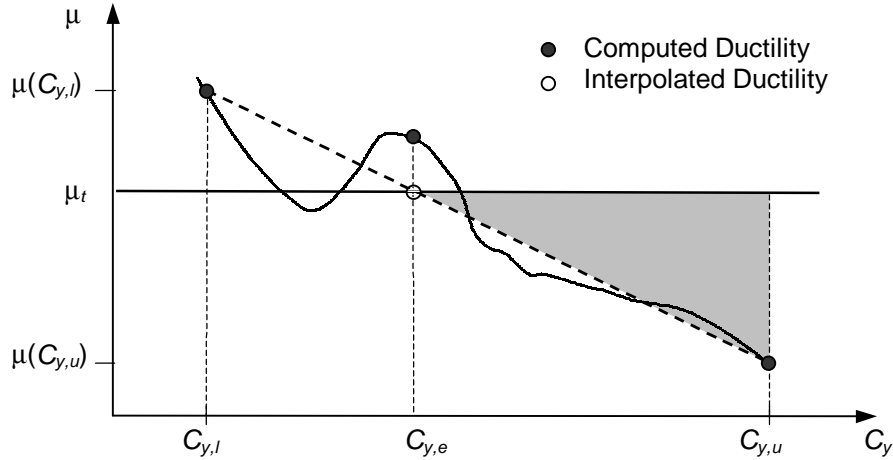


Figure B7. The case where $\mu(C_{y,e}) > \mu_t$

The case $\mu(C_{y,e}) < \mu_t$ is illustrated in Figure B8. This case is more complicated because undulations in the strength-ductility relation might be large enough that a higher-strength solution may exist between $C_{y,e}$ and $C_{y,u}$. The approach taken is to compare the ductilities computed at intermediate strengths with estimates based on linear interpolation between $\mu(C_{y,e})$ and $\mu(C_{y,u})$. A “smoothness ratio” is defined as the ratio e/a , where e = the difference between the interpolated and actual ductilities and a = the difference between the interpolated and target ductilities, as shown in Figure B9. If the smoothness ratio is less than a user-specified “smoothness tolerance” at a sufficient number of points, the strength-ductility relation is considered to be “smooth.” The possibility that an unidentified solution might exist within a region identified as “smooth” is considered to

be remote, because this would require a sharp departure from the interpolated strength-ductility relationship. If the interval between $C_{y,e}$ and $C_{y,u}$ is identified as smooth, it may be rejected from further consideration. Then, the solution bounds are revised by setting $C_{y,u} = C_{y,e}$, and the algorithm restarts with the new bounds.

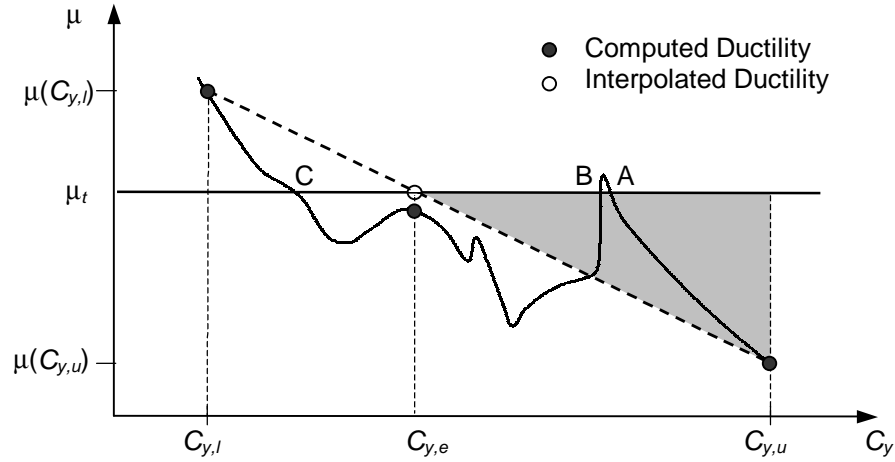


Figure B8. The case where $\mu(C_{y,e}) < \mu_t$

The number of discrete values of C_y that is checked and the allowable deviation of the actual ductility values from the interpolated values impact the efficiency of the algorithm and determine the odds of an unrecognized higher strength solution. Of particular concern is the unusual instance in which the strength-ductility relation happens to coincide with the interpolated ductilities at the chosen values of C_y , but deviates significantly from the interpolated function elsewhere. Considering this possibility, more reliable conclusions may be obtained when several points are checked rather than just one (or two), and checking several points allows the tolerances to be relaxed somewhat relative to cases in which fewer points are checked. Experience indicates that a region may be discarded when the smoothness ratio is less than a smoothness tolerance of 0.20 at three successive points. For this reason, the interval between $C_{y,e} = C_{y,u}$ is divided into 4 segments in Figure B9. The algorithm proceeds sequentially from $C_{y,1}$ to $C_{y,3}$.

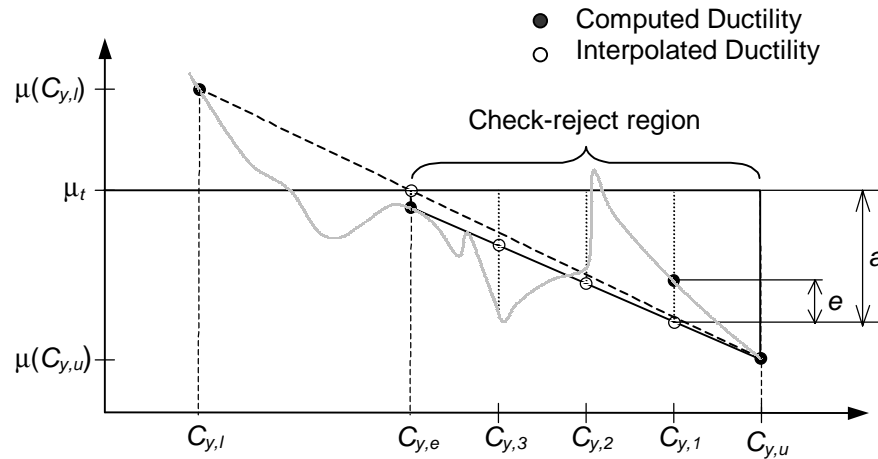


Figure B9. Definition of smoothness ratio (e/a), in the context of checking an interval for rejection

If the smoothness ratio exceeds the smoothness tolerance at any intermediate strength, the possibility that a solution may exist in the vicinity of the current yield strength is pursued further. Figure B10 illustrates this case, for which two additional points are added, each halfway between the current C_y and the closest points on either side. The smoothness of the strength-ductility relation is now evaluated at the original points ($C_{y,1}$, $C_{y,2}$, $C_{y,3}$) and at the added points. The estimated ductilities are now based on linear interpolation, making use of the ductility value that was just determined. In this manner, the interpolation function begins to conform more closely to the actual strength-ductility relation where it previously had violated the smoothness criterion. Note that points are not added if the distance between adjacent points would be less than the specified tolerance on the yield strength coefficient; in this case the algorithm proceeds to the next previously-established point. This process is repeated for each interpolated point until all points between $C_{y,u}$ and $C_{y,e}$ are evaluated.

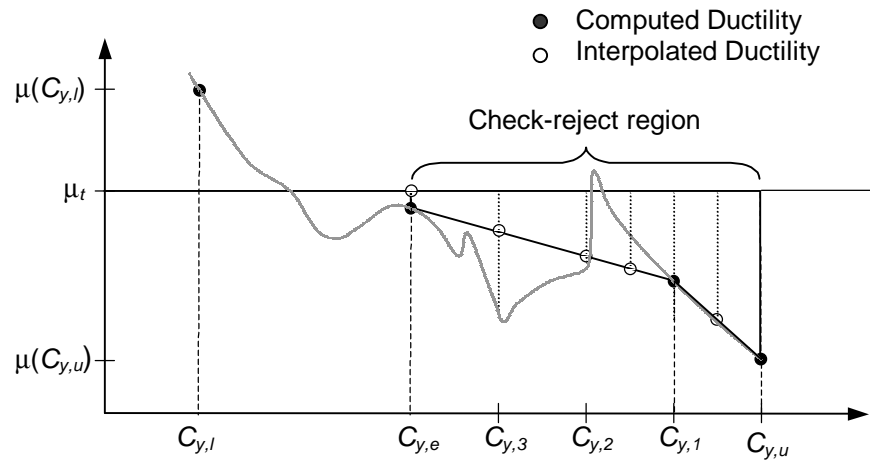


Figure B10. Checking for a possible solution in the check-reject region.

If the ductility computed at an intermediate strength exceeds the target ductility, the process is halted, and new bounds are established by setting $C_{y,l}$ equal to the current yield strength coefficient and setting $C_{y,u}$ to the previous C_y . Because the algorithm works down progressively from $C_{y,u}$, if a ductility is computed that is within the user-specified ductility tolerance, the corresponding C_y is reported as solution.

If the “check-reject” approach determines that the region from $C_{y,u}$ to $C_{y,e}$ can be discarded, then the algorithm restarts with the upper and lower bounds set equal to $C_{y,e}$ and $C_{y,l}$, respectively. This continues until the strength interval between $C_{y,u}$ and $C_{y,l}$ is smaller than a user-specified value or the computed ductility is within a specified percentage of the target ductility. In either of these events, the algorithm switches to the fast search bisection phase.

B.3.2 Fast Search Bisection

The fast search portion of the algorithm assumes the bounds of the solution have been narrowed sufficiently that the first solution obtained within these bounds is the correct solution—that is, a higher strength solution is assumed not to exist. The solution bounds are those determined in the first phase of the algorithm. The flowchart for the fast search interpolation is illustrated in Figure B11. Key points are described in the following.

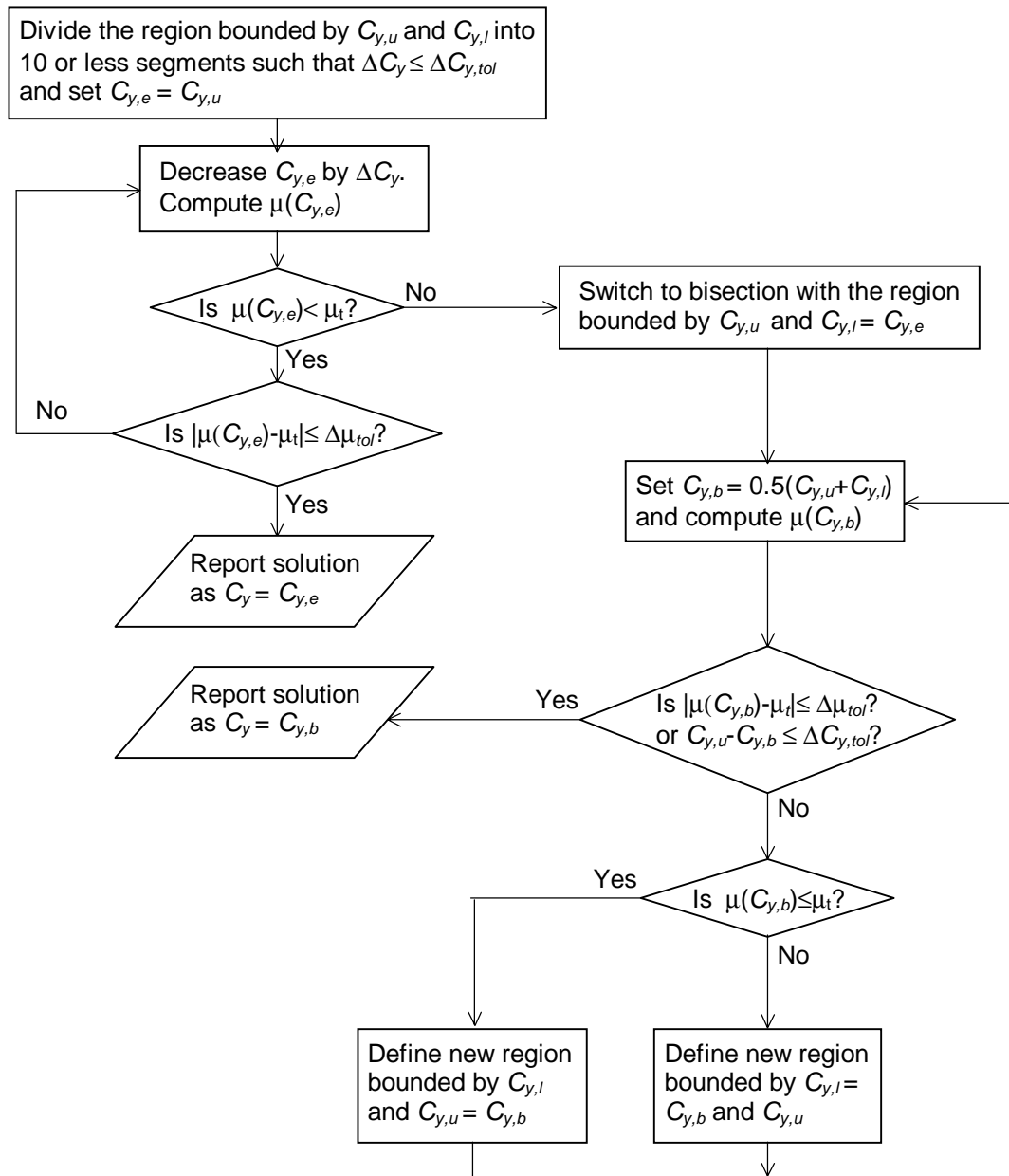


Figure B11. Bisection with the “fast search” algorithm

The fast search algorithm begins by dividing the previously identified solution bounds into 10 segments, if these segments are larger than the specified tolerance on C_y . If not, fewer segments are used, such that each segment is larger than the specified tolerance on C_y . The ductilities corresponding to each strength coefficient are computed, beginning with the largest strength coefficient and stopping when the computed ductility

exceeds the target ductility. The yield strength coefficient corresponding to the larger ductility is assigned to $C_{y,l}$ and the next larger yield strength coefficient is assigned to $C_{y,u}$. The division into as many as 10 segments is not strictly necessary, but was implemented in case the solution bounds determined in the first phase are relatively broad, such as might happen if a user should specify relatively large tolerances.

A bisection procedure is then applied recursively to the two adjacent yield strength coefficients in which a solution lies. The procedure begins with the points $C_{y,l}$ and $C_{y,u}$. The ductility at the point $C_{y,b} = (C_{y,l} + C_{y,u})/2$ is then determined. If the computed ductility is within the ductility tolerance or if the yield strength coefficient is within the tolerance on the yield strength coefficient, then $C_{y,b}$ is reported as the solution. If neither tolerance is satisfied, then the solution must lie between either $C_{y,l}$ and $C_{y,b}$ or $C_{y,b}$ and $C_{y,u}$. If $\mu(C_{y,l}) > \mu_t > \mu(C_{y,b})$, then $C_{y,l}$ is retained and $C_{y,u}$ is reset to $C_{y,b}$. Otherwise, $\mu(C_{y,b}) > \mu_t > \mu(C_{y,u})$, then $C_{y,l}$ is reset to $C_{y,b}$ and $C_{y,u}$ is retained. The bisection procedure is then repeated using the new interval from $C_{y,l}$ to $C_{y,u}$.

Throughout the computations a value of C_y is considered acceptable if the computed ductility is within a specified ductility tolerance of the specified target ductility, to avoid computation that achieves unnecessary precision. A tolerance on yield strength coefficient is also needed, however, because of the possibility that a discontinuity in the strength-ductility relationship is large enough that a solution can not be obtained that satisfies the ductility tolerance. The tolerances on strength and ductility are specified as percentages of the average of $C_{y,l}$ and $C_{y,u}$ and the target ductility, so that their scales are independent of the absolute values of strength and ductility. The average of the lower and upper bound strengths is used because this value becomes a good approximation of the actual solution as the strength interval is reduced.

B.4 Comparison of Results with Other Programs

The present algorithm is implemented in the USEE program. Results obtained with this implementation are compared with those obtained using PCNSPEC (Borosheck, 1991) and BISPEC (Hachem, 2000) for several sample ground motions, listed in Table

B1.¹ Both the computed results and the clock time required for the computations are discussed.

All three programs compute response during successive time intervals using the linear acceleration method, a special case of the Newmark Beta Method (Clough and Penzien, 1993) for which $\alpha=1/2$ and $\beta=1/6$. For each program, a time step of 0.01 sec was specified, although each program may use different subdivisions of this interval as needed to satisfy convergence criteria. All computations were performed for a bilinear load-deformation model on a 300 MHz Pentium II computer with 128 MB RAM running Windows 98.

Table B1. Ground motions used in the computations

Record-ID	Earthquake/Year	Station	Component	PGA (g)
bb92civc360	Big Bear 1992	Big Bear Lake-Civic Center Ground	N360	0.545
ch85lleo010	Chile 1985	Llolleo Basement 1-story bldg	N10	0.712
iv40elcn180	Imperial Valley 1940	El Centro	N180	0.312
mx85sct1270	Mexico City 1985	SCT1-Secretaria Comucinacion	N270	0.171
wh87mtwl090	Whittier 1987	MT. Wilson-Caltech Seismic Station	N90	0.185

B.4.1 Accuracy of Constant Ductility Response Spectra

Constant ductility response spectra were computed for the three programs and the five ground motions of Table B1. Figures B12 and B13 show the response spectra computed for the El Centro and Llolleo records, respectively, for $\mu=2$. The solutions obtained using the three programs were nearly identical, with only a few results obtained from PCNSPEC deviating noticeably from the results obtained with BISPEC and USEE. In these few cases, PCNSPEC missed the highest strength solution, and reported a lower strength solution that resulted in the target ductility. The overall agreement of the solutions indicates that the algorithm implemented in USEE is at least as accurate as those implemented in other available codes.

¹ The program NONLIN was not considered in this comparison because the constant ductility strengths are estimated by linear interpolation between C_y values for $\mu=1$ and $\mu=8$, rather than being computed explicitly for each value of ductility.

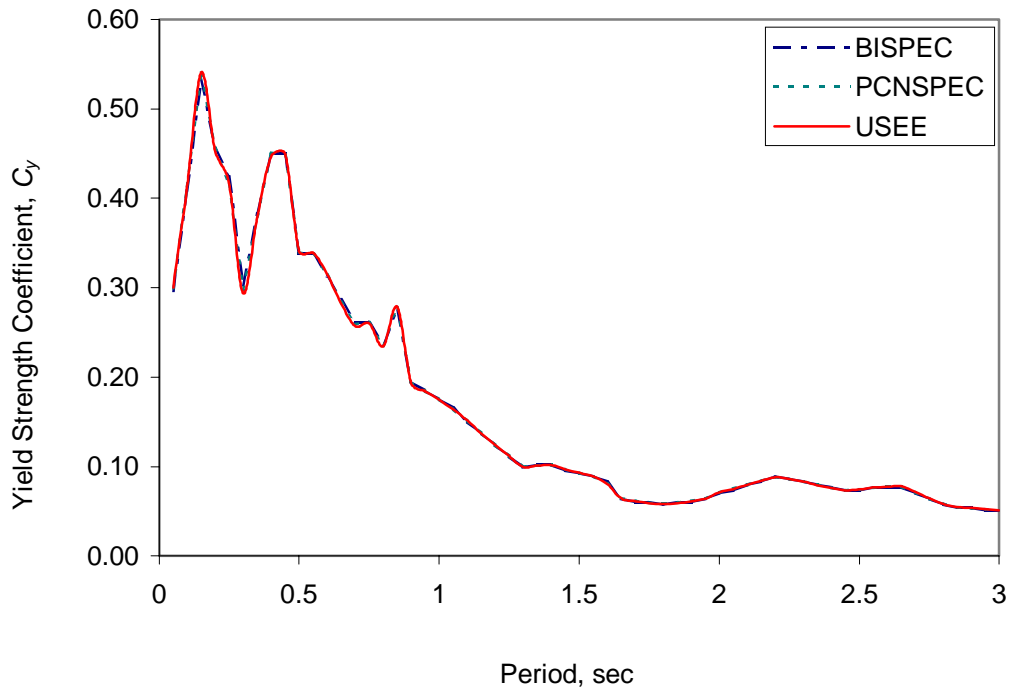


Figure B12. Constant ductility response spectrum for $\mu=2$ for the El Centro record

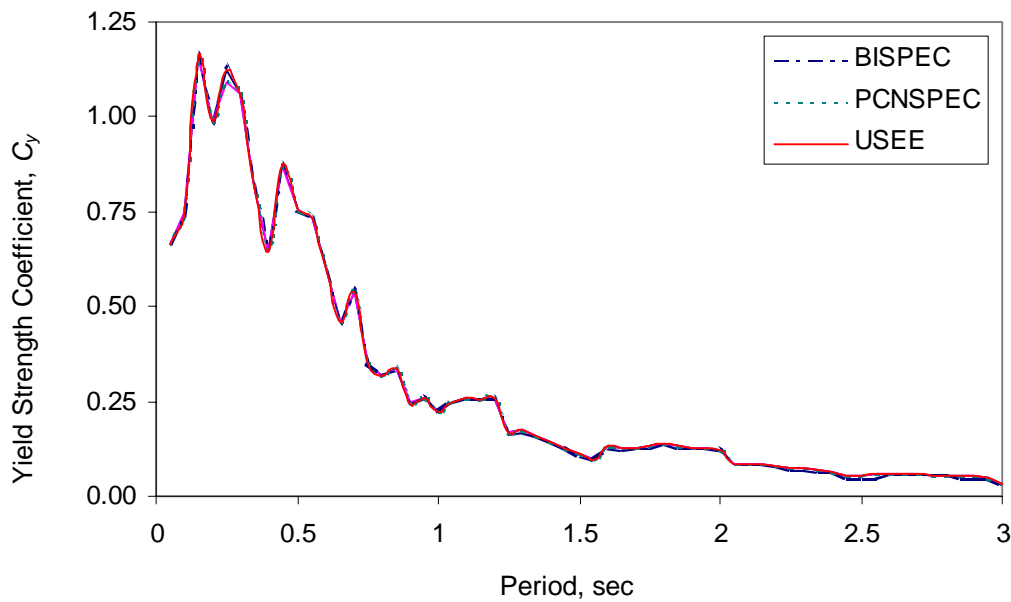


Figure B13. Constant ductility response spectrum for $\mu=2$ for the Llole record.

B.4.2 Computational Efficiency

The clock times required to obtain constant ductility response spectra for $\mu=2$ and $\mu=8$ for the 5 records of Table B1 are reported in Table B2. It is apparent that the USEE

implementation is significantly faster than the other codes, and that the differences are dependent on the ground motion records, to some extent. Many factors may contribute to differences in computation time, including (i) the efficiency of the algorithms for the forward computation; (ii) the efficiency of algorithms used for constant ductility iterations, and (iii) overhead associated with graphical interfaces and (iv) other implementation-specific details. Some of the implementation-specific differences are as follows:

- PCNSPEC requires that the lower and upper bound values of yield strength coefficient be specified, along with the number of intervals within the bounds. These intervals determine the discrete values of C_y that PCNSPEC uses. PCNSPEC then determines a solution within the two adjacent values of C_y on either side of the target ductility. This potentially may result in lower strength solutions or in no solutions at all if the solution lies outside the specified bounds. In this comparison study, the boundaries were defined to include the solution, and the number of intervals is set to 50.
- The same tolerances on strength were specified for USEE and PCNSPEC. Tolerances for BISPEC are set internally and cannot be specified.

Table B2. Clock time required to compute response spectra for different ductilities using different software programs

Record-ID	Computation Time (sec)					
	BISPEC		PCNSPEC		USEE	
	$\mu=2$	$\mu=8$	$\mu=2$	$\mu=8$	$\mu=2$	$\mu=8$
bb92civc360	15	21	17	74	6	7
ch85lleo010	52	111	57	71	24	31
iv40elcn180	5	12	4	36	2	3
mx85sct1270	53	87	21	26	10	12
wh87mtwl090	7	11	95	153	3	4

For the foregoing reasons, one can not conclude from Table B2 that the constant ductility algorithm implemented in USEE is necessarily more efficient than those implemented in other software programs. It is clear, however, that the combination of the constant ductility algorithm, the efficiency of the forward computation, and other

implementation-specific details work together to result in relatively fast computations using USEE.

B.5 Conclusion

An algorithm consisting of an initial bounding of the solution phase and a fast search bisection phase was described. This algorithm was implemented in the USEE program. Comparisons with other programs indicates: (i) the USEE program is at least as accurate as PCNSPEC and BISPEC, and (ii) the USEE computation is relatively fast.

B.6 Glossary/Definitions

Smoothness Ratio (e/a) is the ratio of deviation, e , of the computed ductility value from the value expected based on linear interpolation, to the distance, a , between the target and expected ductilities. See Figure B9.

Smoothness Tolerance is a user-specified non-dimensional value that is compared to the Smoothness Ratio to determine whether the departure from the interpolated ductility is large enough to require further investigation of a possible solution on either side of the current yield strength coefficient.

Tolerance on Target Ductility is a user-specified tolerance that determines whether the current yield strength coefficient may be reported as a solution. If the computed ductility is within the user-specified tolerance from the target ductility, the corresponding C_y is reported as the solution.

Tolerance on Yield Strength Coefficient is a user-specified tolerance that halts the iteration on strength when successive values differ by less than the specified tolerance. The tolerance is specified as a percentage of the average of the two adjacent values of C_y .

Target Ductility is the specified displacement ductility for which the associated yield strength coefficients are determined, by iteration, for each specified period.

Yield Strength Coefficient is the yield strength of a SDOF oscillator normalized by its weight.

APPENDIX C: Notation

a	the distance between the target and expected ductilities
a_I	pulse amplitude (g) when a pulse is used for base motion input
C_y	yield strength coefficient of a SDOF oscillator
C_y^*	yield strength coefficient of a SDOF analogue
$C_{y,e}$	equivalent yield strength coefficient of a SDOF analogue
$C_{y,b}$	yield strength coefficient obtained by bisecting the interval between $C_{y,u}$ and $C_{y,l}$
$C_{y,e}$	expected yield strength coefficient of a SDOF oscillator obtained by interpolation between $C_{y,u}$ and $C_{y,l}$
$C_{y,i}$	yield strength coefficient at point i
$C_{y,l}$	lower bound of C_y interval, for which the corresponding peak displacement ductility, μ , is larger than the target ductility, μ_t
$C_{y,u}$	upper bound of C_y interval, for which the corresponding peak displacement ductility, μ is smaller than the target ductility, μ_t
c_c	critical damping
E_a	absorbed energy
E_h	irrecoverable hysteretic energy
E_i	relative input energy
E_k	relative kinetic energy
E_ξ	energy dissipated by viscous damping
E_s	recoverable elastic strain energy
e	deviation of the computed ductility value from the value expected based on linear interpolation
F_y	yield strength of a SDOF oscillator
F_y^*	equivalent yield strength of a SDOF analogue
k	initial stiffness of a SDOF oscillator
f	frequency of vibration of a SDOF oscillator
g	acceleration due to gravity
K	tangent stiffness of a SDOF oscillator
K^*	equivalent tangent stiffness of a SDOF analogue
M	mass of a SDOF oscillator
M^*	equivalent mass of a SDOF analogue
P	applied force to a SDOF oscillator
$P(t)$	applied force to a SDOF oscillator at time t
Q	vector of story forces at the floor levels for a multistory building
$Q(t)$	vector of story forces at the floor levels for a multistory building at time t
Q^*	vector of equivalent story forces at the floor levels of a SDOF analogue of a multistory building
$Q^*(t)$	vector of equivalent story forces at the floor levels of a SDOF analogue of a multistory building at time t
R	strength reduction factor
R	restoring force of a SDOF oscillator
$R(t)$	restoring force of a SDOF oscillator at time t
r	geometric ratio used for the specification of non-uniformly spaced periods
S_a	pseudo-acceleration
S_d	peak spectral displacement

T	initial (elastic) period of vibration as a function of the initial stiffness, k and mass, m
T_i	initial (elastic) period of vibration of the i^{th} mode of a multistory building
t	time
t_I	pulse duration when a pulse is used for base motion input
t_{RD}	pulse record duration when a pulse is used for base motion input
tol	convergence tolerance (as a % of the yield displacement)
u	displacement of a system relative to the ground
$u(t)$	displacement of a system relative to the ground at time t
u_g	displacement of the ground relative to a fixed datum
$u_g(t)$	displacement of the ground relative to a fixed datum at time t
u^t	total displacement of the system
$u^t(t)$	total displacement of the system at time t ($u^t(t)=u(t)+u_g(t)$)
\dot{u}_g	velocity of the ground with respect to a fixed datum
$\dot{u}_g(t)$	velocity of the ground with respect to a fixed datum at time t
\ddot{u}_g	acceleration of the ground with respect to a fixed datum
$\ddot{u}_g(t)$	acceleration of the ground with respect to a fixed datum at time t
u_{roof}	roof displacement with respect to the ground
$u_{roof}(t)$	roof displacement with respect to the ground at time t
u_y	yield displacement of a SDOF oscillator
u_y^*	equivalent yield displacement of SDOF analogue
V_y	base shear strength of a SDOF oscillator
V_y^*	equivalent base shear strength of the SDOF analogue
W	weight of a SDOF oscillator.
W^*	equivalent weight of SDOF analogue
α_i	mass participation factor for mode i
α	ratio of post-yield stiffness to initial stiffness
α, β	Newmark Beta Method parameters
Γ_i	participation factor for mode i
Δ_c	static collapse displacement
Δ_y	yield displacement of a SDOF oscillator
Δ_u	ultimate displacement of a SDOF oscillator
$\Delta C_{y,tol}$	tolerance on yield strength coefficient
Δt	time interval
$\Delta u(t)$	incremental displacement at time t
$\Delta \dot{u}(t)$	incremental velocity at time t
$\Delta \ddot{u}(t)$	incremental acceleration at time t
$\Delta R(t)$	incremental restoring force of a SDOF oscillator at time t
$\Delta P(t)$	incremental applied force to a SDOF oscillator at time t
$\Delta \tau$	user specified time step
δ	displacement difference
μ	peak displacement ductility
μ_t	target displacement ductility

μ_{tol} tolerance on target ductility
 ξ critical damping ratio
 ϕ first mode displaced shape vector of a MDOF system
 ω^* equivalent circular frequency of SDOF analogue

APPENDIX D: USEE Organization

The organization of the Visual Basic code of USEE is described for documentation purposes. The VB interface consists of Forms, Modules and Help Files. The Forms and Modules and their functions are described below.

Forms

1. Main form, displays main window.
2. Copyright and agreement of terms form.
3. About USEE form, displayed in **Help About USEE**.
4. Base Input form, contains Recorded Ground Motions, Synthetic Motions and Pulse input motions for SDOF, Approximate Multistory Building, and Response Spectra Modules.
5. Structural Properties form for SDOF analysis and Multistory Building Approximation analysis, contains structural properties input for the SDOF, Multistory Building Approximation Modules.
6. Structural Properties form for Response Spectra analysis contains structural properties input for Response Spectra Modules.
7. Manual Testing for Load-Deformation Models form.
8. Multistory Description form.
9. File Header View form.
10. Unit Types form.
11. Summary Log for the current session form.
12. Zoom Plots Form.
13. View SDOF Results form.
14. View Multistory Approximation Results form.
15. View Response Spectra Results form.
16. Compare SDOF and Multistory Building Approximation analysis Results form.
17. Options and user preferences form.

Modules

1. Input Preparation module.
2. SDOF and Multistory Building Approximation analysis module.
3. Response Spectra analysis module.

4. File Operation module.
5. Current Analysis File Handling module.
6. Plotting module.
7. Internet Access module.
8. Help File Connectivity module.
9. Exporting SDOF and MDOF module.
10. Error checking and handling module.
11. Error throwing module.

APPENDIX E: References

Abrams, D.P., *Nonlinear Earthquake Analysis of Concrete Building Structures*, Final Report on a Study to the American Society for Engineering Education Postdoctoral Fellowship Program, September 1985.

ATC-40, *Seismic Evaluation and Retrofit of Concrete Buildings, Volumes 1 and 2*, Applied Technology Council, November 1996. Report No. SSC 96-01.

Black E., and Aschheim, M., 2000, *Seismic Design and Evaluation of Multistory Buildings Using Yield Point Spectra*, CD Release 00-04, Mid-America Earthquake Center, University of Illinois, Urbana, September.

Boroschek, R.L., and Mahin, S.A., *PCNSPEC Manual, A Modified Version of NONSPEC*, 1991 (unpublished).

Charney, F., *Nonlinear Dynamic Time History Analysis of Single Degree of Freedom Systems (NONLIN), Version 6.01*, Advanced Structural Concepts, Inc., Golden, Colorado, and Schnabel Engineering, Denver, Colorado under a contract with Federal Emergency Management Agency, 1998. Also available from <http://www.fema.gov/emi/nonlin.htm>

Chopra, A., *Dynamics of Structures. Theory and Applications to Earthquake Engineering*, Prentice-Hall, Inc., New Jersey, 1995.

Clough, R.W., and Penzien, J., *Dynamics of Structures*, 2nd Edition, McGraw-Hill, Inc, New York, 1993.

Fajfar, P., and Fischinger, M., “N2 – A Method for Non-Linear Seismic Analysis of Regular Structures,” *Proceedings from the Ninth World Conference on Earthquake Engineering*, Tokyo-Kyoto, Japan, 1988.

FEMA-273, *NEHRP Guidelines for the Seismic Rehabilitation of Buildings*, Report No. FEMA-273, Federal Emergency Management Agency, Washington D.C., May 1997.

FEMA-274, *NEHRP Commentary on the Guidelines for the Seismic Rehabilitation of Buildings*, Report No. FEMA-274, Federal Emergency Management Agency, Washington D.C., October 1997.

Hachem, M.M., BISPEC Version 1.1.2, University of California, Berkeley, 2000. Available from <http://www.ce.berkeley.edu/~hachem/bispec/index.html>

Lawson, R.S., Vance, V., and Krawinkler, H., “Nonlinear Static Push-Over Analysis – Why, When, and How?”, *Proceedings of the Fifth U.S. Conference in Earthquake Engineering*, Earthquake Engineering Research Institute, Oakland, California, 1994.

Mahin, S.A., and Bertero, V.V., “An Evaluation of Inelastic Design Spectra,” *Journal of Structural Engineering*, ASCE, Vol. 107, No. ST9, September 1981.

Mahin, S.A., and Lin, J., *Construction of Inelastic Response Spectra for Single-Degree-of-Freedom Systems*, Report No. UCB/EERC-83/17, Earthquake Engineering Research Center, Berkeley, California, 1983.

Miranda, E., *Seismic Evaluation and Upgrading of Existing Buildings*, Ph.D. dissertation, Department of Civil Engineering, University of California, Berkeley, California, 1991.

Newmark, N.M., "A Method of Computation for Structural Dynamics," *Journal of the Engineering Mechanics Division, ASCE*, Vol. 85, No. EM 3, July 1959.

Newmark, N.M, and Hall, W.J., *Seismic Design Criteria for Nuclear Reactor Facilities*, Technology Report 4, Building Practices for Disaster Mitigation, National Bureau of Standards, U.S. Department of Commerce, 1973.

Newmark, N.M., and Riddell, R., "Statistical Analysis of the Response of Nonlinear Systems Subjected to Earthquakes," *Civil Engineering Studies, Structural Research Series*, No. 468, University of Illinois, Urbana. August 1979.

Petkov, Z. B.; Ganchev, S. G., "An algorithm for computation of inelastic response spectra," *Proceedings of the Eleventh European Conference on Earthquake Engineering*, A. A. Balkema, Rotterdam, 1998.

Prakash, V., Powell, G.H., and Campbell, S., 1993, *Drain-2DX Base Program Description and User Guide*, Report No. UCB/SEMM-93/18, Structural Engineering Mechanical and Materials, Berkeley, California, 1993.

Qi, X., and Moehle, J.P., *Displacement Design Approach for Reinforced Concrete Structures Subjected to Earthquakes*, Report No. EERC 91/02, Earthquake Engineering Research Center, Berkeley, California, 1991.

Saiidi, M., and Sozen, M.A., "Simple Nonlinear Seismic Analysis of R/C Structures," *Journal of Structural Division, ASCE*, 1981, Vol. 107, No. ST5.

Uang, C. M., and Bertero, V. V., *The Use of Energy as a Design Criterion in Earthquake Resistant Design*, Report No. UCB/EERC-88/18, Earthquake Engineering Research Center, Berkeley, California, Nov. 1988.

Vidic, T., Fajfar, P., Fischinger, M., "Consistent Inelastic Design Spectra: Strength and Displacement," *Earthquake Engineering and Structural Dynamics*, vol. 23, pp507-521, 1994.

Wilson, E.L., Farhoomand, I., and Bathe, K.J., "Nonlinear Dynamic Analysis of Complex Structures," *Earthquake Engineering and Structural Dynamics*, 1973, Vol. 1, pp. 241-252.

Wen, Y.K. and Chiun-Lin Wu, Project RR-1 of the Mid America Earthquake Center, 1999.